$SU(4)$ symmetry for strongly correlated electrons: Kondo and mixed-valence effects in terms of Gell-Mann matrices

K. Kikoin

Raymond and Beverly Sackler Faculty of Exact Sciences, School of Physics and Astronomy, Tel-Aviv University, Tel-Aviv 69978 Israel

(Received 25 November 2011; revised manuscript received 5 February 2012; published 18 May 2012)

The concept of dynamical symmetries is used for formulation of the renormalization group approach to the Kondo effect in the Anderson model with repulsive and attractive interaction U in the Kondo and mixed valence regimes. It is shown that the generic local dynamical symmetry of the Anderson Hamiltonian is determined by the $SU(4)$ Lie group. The Anderson Hamiltonian is rewritten in terms of the Gell-Mann matrices of fourth rank, which form the set of group generators and the basis for construction of the irreducible vector operators describing the excitation spectra in the charge and spin sectors. The multistage Kondo screening is interpreted as a consecutive reduction of local $SU(n)$ dynamical symmetries from $SU(4)$ to $SU(2)$. It is shown that the similarity between the conventional Kondo cotunneling effect for spin $1/2$ in the positive U model and the Kondo resonance for pair tunneling in the negative U model is a direct manifestation of implicit $SU(4)$ symmetry of the Anderson/Kondo model. The relations between the local $SU(4)$ dynamical symmetry and the global $SO(4)$ symmetry in the Hubbard model are discussed in brief.

DOI: 10.1103/PhysRevB.85.195132 PACS number(s): 02.20.Qs, 05.10.Cc, 73.21.La

I. INTRODUCTORY REMARKS

In the 60's and 70's, when the basic concepts of dynamical symmetries have been formulated and elaborated,[1–6] only few physical realizations of these symmetries could be found in the realm of existing quantum mechanical objects (see Refs. 7 and 8 for a review). One may mention the hydrogen atom[9–11] and the harmonic oscillator in various spatial dimensions[12–14] as systems for which the study of their dynamical symmetries revealed additional facets of excitation spectra and response to external fields. Rapid progress in the nanotechnology and nanophysics during the two recent decades significantly extended the field of applicability of these concepts and enriched the theory with some new ideas.

Contemporary nanophysics[15–19] deals with the artificial structures that consist of a finite number of electrons confined within a tiny region of space, where the energy spectrum of electrons is discrete. As a result, such objects can be treated as "zero-dimensional" artificial atoms or molecules with spatially quantized discrete states, well defined symmetry, and controllable electron occupation. Besides, modern technologies allow fabrication of devices where a "natural" atom or molecule is spatially separated from the rest of a device, so that the physical properties of an *individual* atom or atomic cluster may be studied experimentally.

In this paper, we analyze the dynamical symmetries that arise in a framework of group theoretical approach to a few-electron nanosystem $\mathcal{S}$ with definite symmetry $\mathsf{G}_{\mathcal{S}}$ in a contact with a macroscopic system $\mathcal{B}$ ("bath" or "reservoir"). Due to this contact, the symmetries of the system $\mathcal{S}$ and the corresponding conservation laws are violated. If the contact between two systems is weak enough, the dynamics of interaction may be described in terms of transitions between the eigenstates of a system $\mathcal{S}$ belonging to different irreducible representations of the group $\mathsf{G}_{\mathcal{S}}$ generated by the operators which obey the algebra $\mathsf{g}_{\mathcal{S}}$. If the operators describing transitions between these eigenstates together with generators of the group $\mathsf{G}_{\mathcal{S}}$ form the enveloping algebra $\mathsf{d}_{\mathcal{S}}$ for the algebra $\mathsf{g}_{\mathcal{S}}$, one may say that the system $\mathcal{S}$ possesses a dynamical symmetry characterized by some group $\mathsf{D}_{\mathcal{S}}$. The dynamical symmetry group technique offers mathematical tools for the unified approach to quantum objects, which allows one to consider not only the spectrum of a system $\mathcal{S}$, but also its response to external perturbation violating the symmetry $\mathsf{G}_{\mathcal{S}}$ and various complex many-body effects characterizing the interaction between the system $\mathcal{S}$ and its environment $\mathcal{B}$. We discuss a general algorithm of dynamical symmetry group approach to the system $\mathcal{B}+\mathcal{S}$ and its practical application to the single-electron tunneling in complex quantum dots and single-molecule transistors. This tunneling is described in the framework of Anderson model with repulsive and attractive interaction between the confined electrons.

It will be shown that the dynamical symmetry group describing all transitions between the spin and charge states in the subsystem $\mathcal{S}$ (e.g., quantum dot under Coulomb blockade) with variable occupation numbers $\mathcal{N}=0,1,2$ is the semisimple Lie group $SU(4)$. The basic matrix representation for the generators of this group is formed by 15 Gell-Mann matrices of 4th rank. The Anderson Hamiltonian describing electron tunneling between the dot and the bath will be rewritten in terms of these matrices. To demonstrate this formalism afoot, we will reinterpret the renormalization group (RG) approach to the Anderson-Kondo problem[20–24] in terms of reduced dynamical $SU(n)$ symmetries. Both the high energy/weak coupling RG description of T matrix and the low-energy/strong coupling Bethe ansatz for scattering matrix[25,26] may be formulated in terms of corresponding Gell-Mann operators. The well-known duality of Kondo effect in the Anderson model with repulsive and attractive interaction[27,28] also stems from the internal structure of the Gell-Mann matrices. Then we discuss the manifestations of $SU(4)$ dynamical symmetry in the mixed valence regime with completely suppressed spin excitations. Finally, we will show that the Gell-Mann operators are hidden in the regular states forming the basis for the Bethe-Ansatz solution of the one-dimensional Hubbard chain.[29]

II. HUBBARD OPERATORS GENERATING THE SPECTRUM OF NANOOBJECT

Following the definition used in Ref. 11, we define the dynamical symmetry group $\mathsf{D}_{\mathcal{S}}$ as a Lie group of finite dimension characterized by the irreducible representations that act in the whole Hilbert space of eigenstates $|l\lambda\rangle$ of the Schrödinger equation

$$\hat{H}|l\lambda\rangle = E_l|l\lambda\rangle \tag{2.1}$$

describing the quantum system $\mathcal{S}$. Here, l is the index of irreducible representation and λ enumerates the lines of this representation. The projection operators

$$X_{(l)}^{\lambda\mu} = |l\lambda\rangle\langle l\mu| \tag{2.2}$$

play the central part in the procedure of construction of irreducible representations l of the group of Schrödinger equation $\mathsf{G}_{\mathcal{S}}$. The basic property of these operators is given by the equation

$$X_{(l)}^{\lambda\mu}|l'\nu\rangle = \delta_{ll'}\delta_{\mu\nu}|l\lambda\rangle\,. \tag{2.3}$$

One may add to the set (2.2) the operators

$$X_{(ll')}^{\lambda\mu} = |l\lambda\rangle\langle l'\mu|, \tag{2.4}$$

which project the states belonging to different irreducible representations ($l \neq l'$) of the group G_{S} one onto another. These operators may be also used for construction of the Lie algebras $\mathsf{d}_{\mathcal{S}}$ generating the spectrum of eigenstates of the Schrödinger equation and transitions between these states. Unifying the notations $|l\lambda\rangle = \Lambda\rangle$, we obtain the commutation relations

$$[X^{\Lambda\Lambda'}, \hat{H}] = (E_{\Lambda'} - E_{\Lambda})\hat{H}. \tag{2.5}$$

The right-hand side of Eq. (2.5) turns into zero provided the states Λ and Λ' belong to the same irreducible representation of the group $\mathsf{G}_{\mathcal{S}}$

The operators $X^{\Lambda_1\Lambda_2}$ have been exploited by J. Hubbard as a convenient tool for description of elementary excitations in strongly correlated electron systems (SCES). His seminal model of interacting electron motion in a narrow band, known now as the Hubbard model[30–33] was the first microscopic model of SCES for which the conventional perturbative approach based on the Landau Fermi liquid hypothesis turned out to fail. Now the realm of SCES is really vast, and the most of artificial nanostructures in fact belong to this realm. In particular, complex quantum dots under strong Coulomb blockade are typical examples of short Hubbard chains or rings.

If a closed algebra $\mathsf{d}_{\mathcal{S}}$ exists for the set of Hubbard operators (2.2) and (2.4), then one may state that the system described by the Hamiltonian (2.1) possesses the dynamical symmetry $\mathsf{D}_{\mathcal{S}}$. This algebra is conditioned by the norm

$$\sum_{\Lambda} X^{\Lambda\Lambda} = 1 \tag{2.6}$$

and by the commutation relations for the operators $X^{\Lambda_1\Lambda_2}$. In the general case, these relations may be presented in the following form:[33]

$$[X^{\Lambda_1\Lambda_2}, X^{\Lambda_3\Lambda_4}]_{\mp} = X^{\Lambda_1\Lambda_4}\delta_{\Lambda_2\Lambda_3} \mp X^{\Lambda_3\Lambda_3}\delta_{\Lambda_1\Lambda_4}. \tag{2.7}$$

The "general case" implies that the Fock space includes the states that may belong to different charge sectors, i.e., changing the state Λ_1 for the state Λ_2 means changing the number of fermions $\mathcal{N}_{\Lambda_2} \to \mathcal{N}_{\Lambda_1}$ in the many-particle system. If both $\mathcal{N}_{\Lambda_1} - \mathcal{N}_{\Lambda_2}$ and $\mathcal{N}_{\Lambda_3} - \mathcal{N}_{\Lambda_4}$ are odd numbers (Fermi-type operators), the plus sign should be chosen in Eq. (2.7). If at least one of these differences is zero or an even number (Bose-type operators), one should take the minus sign.

Thus the operators $X^{\Lambda\Lambda'}$ form a closed algebra. In particular, the Hubbard operators for the Hubbard model form the $Spl(2,1)$ superalgebra (2.7) which has been used, e.g., for construction of solutions of the reduced version of the original Hubbard model, namely, for the 1D t-J model.[34,35] In this paper, we discuss another possibility of using the operators $X^{\Lambda\Lambda'}$ in the studies of excitation spectra in SCES. If the Hamiltonian of such system has the form $\hat{H} = \hat{H}_0 + \hat{H}'$, where the spectrum E_{Λ} of correlated electrons described by the Hamiltonian $\hat{H}_0$ is exactly known, the Hubbard operators describing the interlevel transitions provide a convenient tool for construction of the algebras generating the dynamical symmetry group $\mathsf{D}_{\mathcal{S}0}$ of the Schrödinger operator $(\hat{H}_0 - E)$ or the resolvent operator $\hat{\mathsf{R}} = (\hat{H}_0 - E)^{-1}$. Usually, the perturbation term $\hat{H}'$ also contains some generators of $\mathsf{D}_{\mathcal{S}0}$. This perturbation either conserves or violates the local dynamical symmetry, and in some special cases it incorporates $\mathsf{D}_{\mathcal{S}0}$ to another (global) dynamical symmetry $\mathsf{D}_{\mathcal{S}g}$. All three possibilities will be exemplified below.

The generators of the group $\mathsf{D}_{\mathcal{S}0}$ are certain linear combinations of operators $X^{\Lambda\Lambda'}$. The Hubbard operators also may be used for construction of irreducible tensor operators $\mathcal{O}^{(r)}$ (scalars, $r = 0$, vectors, $r = 1$, and tensors $r = 2,3,\ldots$) that transform along the representations of the group $\mathsf{D}_{\mathcal{S}0}$:

$$\mathcal{O}_{\varrho}^{(r)} = \sum_{\Lambda\Lambda'}\langle\Lambda|\mathcal{O}_{\varrho}^{(r)}|\Lambda'\rangle X^{\Lambda\Lambda'}. \tag{2.8}$$

Here, the index ϱ stands for the components of irreducible tensor operator of the rank r. On one hand, it is clear that the operators $X^{\Lambda\Lambda'}$ generate all the eigenstates of the Hamiltonian $\hat{H}_0$ from any given initial state Λ'. On the other hand, the components of the operator $\mathcal{O}^{(r)}$ form their own closed algebra, which characterizes the dynamical symmetry group provided the Hamiltonian $\hat{H}_0$ possesses such symmetry. Having in mind the application of this technique to the geometrically confined nano-objects, we restrict ourself by the discrete eigenstates.

The Clebsch-Gordan expansion (2.8) is the basic equation that allows one to treat the dynamical symmetries of nano-objects in a systematic way. The principal difference between the dynamical symmetries of SCES and those of integrable models is that in the latter case, the spectrum of the object and its dynamical symmetries are known exactly, while in the former case, as a rule, only some part of excitation spectra (usually its lower part) may be found analytically and classified by symmetry. This means that one may judge about the dynamical symmetry of the spectrum only within the definite energy interval $\mathcal{E}$. Respectively, the characteristic energy scale may be different for different problems.

Our main subject is the Kondo effect in quantum dots described by the Anderson Hamiltonian.[36,37] The hierarchy of the energy scales in this problem is well known.[38,39] The

Kondo effect arises as a result of orthogonality catastrophe in the Anderson model,[40] where the conduction electrons in the Fermi sea of metallic electrodes play part of the subsystem $\mathcal{B}$ and the strongly correlated electrons in the quantum dot represent the subsystem $\mathcal{S}$. The largest energy scales in the Anderson model are the width of conduction band D in the subsystem $\mathcal{B}$ and the energy of Coulomb blockade Q in the subsystem $\mathcal{S}$. The electrons confined in the nano-object (quantum dot) are characterized by the ionization energy ϵ_i. Next in the hierarchy of energies are the tunneling amplitude V and the tunneling rate $\Gamma = \pi\rho_0 V^2$ characterizing the process of electron tunneling through the potential barrier, which separates two subsystems. Here, ρ_0 is the density of electron states at the Fermi level ε_F of the electron liquid in the leads. The Kondo effect arises in the single-electron tunneling regime under the restrictions of strong Coulomb blockade Q. In this regime, the charge transport between the source and drain electrodes constituting the subsystem $\mathcal{B}$ is realized as the electron cotunneling, where an electron from the source may tunnel into the dot $\mathcal{S}$ only provided another electron leaves the dot for the drain. Cotunneling, which arises in the fourth order in V, is characterized by the energy J. Finally, the energy scale of Kondo effect $E_K \sim \sqrt{D\Gamma}\exp(-1/\rho_0 J)$ characterizes the crossover from the weak coupling regime $J \ll 1$ to the strong coupling, where J is enhanced due to the multiple creation of low-energy electron-hole pairs in the leads in the process of cotunneling. The Kondo energy also scales the excitations above the ground "Kondo-singlet" state.[38,39] The hierarchy of all these energies is

$$D, U \gg \epsilon_i \gg V \gg \Gamma \gg J \gg E_K. \tag{2.9}$$

An effective way to describe the crossover from the weak to the strong coupling Kondo regime is the renormalization group (RG) approach.[20–24] In this method, the renormalization of parameters ϵ_i, Γ, J in Eq. (2.9) in the course of reduction of the energy scale $\mathcal{E}$ from high energies $\sim D, U$ to low energies still exceeding E_K is calculated. Our purpose is to describe this procedure in terms of dynamical symmetries *that change in the course of reduction of the energy scale* $\mathcal{E}$. It was noticed that the multistage Kondo screening predetermines the nonuniversal features of the Kondo tunneling in the quantum dots with even occupation.[41–43] In that case, the relevant dynamical symmetry groups are $SO(n)$ with $n = 4$–8.[43,44] In this paper, we will show that this language is useful already in the studies of the "ordinary" Kondo effect for quantum dots with odd electron occupation $\mathcal{N}$ characterized by spin $1/2$. The relevant Lie groups are $SU(n)$ with $n = 3,4$.

III. DYNAMICAL SYMMETRIES IN THE ANDERSON MODEL FOR QUANTUM DOTS

As was mentioned above, the dynamical symmetries of confined electrons in the quantum dot $\mathcal{S}$ are revealed in its interaction with the "Fermi bath" $\mathcal{B}$ of conduction electrons. The Anderson Hamiltonian describing the coupling between two subsystems reads

$$\hat{H} = \hat{H}_d + \hat{H}_b + \hat{H}_{db}, \tag{3.1}$$

where three terms describe the nano-object, the Fermi bath, and their coupling, respectively. The term $\hat{H}_{db}$ in general case includes the direct coupling (quantum tunneling of electrons between two subsystems), the direct interaction of Coulomb and exchange nature, and the indirect (kinematic) interaction induced by the tunneling. If the symmetry of nano-object is well defined, the Hamiltonian $\hat{H}_d$ may be diagonalized by means of projection operators (2.2), and the generators of dynamical symmetry group (2.8) arise in the interaction term $\hat{H}_{db}$ in combination with the operators describing the excitations in the Fermi bath. These symmetries cannot be treated in the same way as the symmetries of the integrable systems discussed in the monographs, Refs. 7, 8, and the references therein, because the interaction not only activates the symmetry $\mathsf{D}_\mathcal{S}$ of the nano-object but also involves the charge, orbital, and spin degrees of freedom of the bath. This principal difference was pointed out in Ref. 43, where the quantum tunneling through an artificial molecule (double quantum dot) with even electron occupation $\mathcal{N} = 2$ in presence of the many-particle interaction of Kondo type was described by means of the generators of the $SO(4)$ group.

To take the dynamical symmetries explicitly in the calculations of excitation spectra and in the studies of spin and charge transport in nano-object, one should adhere to the following paradigm:[45] (1) when diagonalizing $\hat{H}_d$ use the projection operators in accordance with Eqs. (2.1)–(2.5); (2) construct the operators $X^{\Lambda\Lambda'}$, which describe transitions between all the states in the "supermultiplet" of eigenstates of $\hat{H}_d$ belonging both to the same and to the different irreducible representations of the symmetry group $\mathsf{G}_\mathcal{S}$ of the Hamiltonian $\hat{H}_d$ and determine the relevant closed algebra generating the dynamical symmetry group $\mathsf{D}_\mathcal{S}$; (3) rewrite $\hat{H}_{db}$ in terms of the configuration change operators (2.4) belonging to adjacent charge sectors $\mathcal{N} \to \mathcal{N} \pm 1$; (4) when projecting the original Anderson Hamiltonian (3.1) on the subspace of low-energy states $\langle\bar{\Lambda}|\ldots|\bar{\Lambda}\rangle$ by means of the Schrieffer-Wolff (SW) transformation[46] or its generalizations, express the Hubbard operators that arise in this transformation via the generators of corresponding dynamical symmetry group using expansion (2.8).

To demonstrate this paradigm in action, let us consider the textbook example of a cell that may contain zero, one, or two electrons with zero orbital moment. The Hamiltonian of this toy model,

$$\hat{H}_d = \epsilon_d \sum_{\sigma=\uparrow,\downarrow} d_\sigma^\dagger d_\sigma + U n_{d\uparrow} n_{d\downarrow}, \tag{3.2}$$

is nothing but the single-site Hamiltonian describing the elementary cell of the nondegenerate Hubbard model[30] with variable occupation number $\mathcal{N} = 0,1,2$ ("Hubbard atom"). Using definition (2.4) of the Hubbard operator, we rewrite $\hat{H}_d$ in the universal form

$$\hat{H}_d = \sum_\Lambda E_\Lambda X^{\Lambda\Lambda}, \tag{3.3}$$

where $\Lambda = 0,\sigma,2$ and the energy levels E_Λ are

$$E_0 = 0, E_\uparrow = E_\downarrow = E_1 \equiv \epsilon_d, E_2 = 2\epsilon_d + U. \tag{3.4}$$

It is convenient to arrange the energy levels in accordance with the available charge and spin sectors [see Fig. 1(a)]. The arrows connecting the levels E_Λ and $E_{\Lambda'}$ correspond to the Hubbard operator $X^{\Lambda\Lambda'}$ and its complex conjugate.

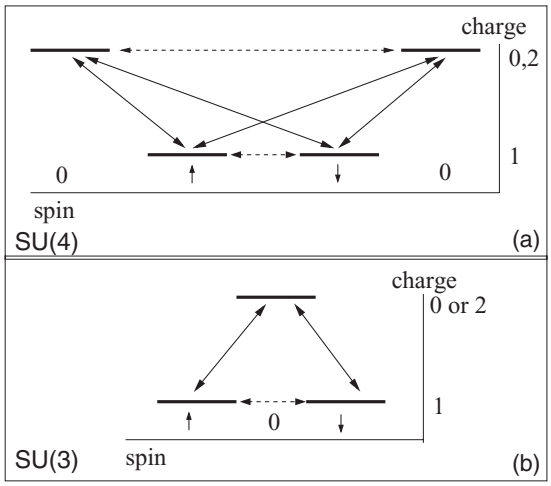

FIG. 1. (a) Scheme of the energy levels for a Hubbard atom with the $SU(4)$ dynamical symmetry describing transitions between the states with occupation $\mathcal{N} = 0,1,2$. (b) The same for a reduced spectrum with the $SU(3)$ dynamical symmetry describing transitions between the states with $\mathcal{N} = 0$ or 2 and $\mathcal{N} = 1$. The Bose-like transitions with even $\delta\mathcal{N} = 0, \pm 2$ are marked by the dashed arrows, the Fermi-like transitions with odd $\delta\mathcal{N} = \pm 1$ are marked by the solid arrows.

This scheme visualizes the Fermi-like and Bose-like operators (solid and dashed lines, respectively), which obey the commutation relations (2.7). There are 15 Hubbard operators describing transitions in this four-level system. The complex matrices of 4th rank describing the transitions between all four levels represent the Lie group $SU(4)$, and the Hubbard operators performing these transitions may be regrouped into the basic matrices of this group, known as the Gell-Mann matrices $\lambda_1 - \lambda_{15}$ (see Appendix). Thus the generic dynamical symmetry of Hubbard atom that is realized within the energy interval $\mathcal{E} \sim U, D$ is $SU(4)$.

Reduction of the energy scale to the interval $\epsilon_i < \mathcal{E} \ll U$ results in quenching the doubly occupied levels. We remain with a three-level symmetry, and the dynamical symmetry reduces from $SU(4)$ to $SU(3)$ [see Fig. 1(b)]. The algebra generating this group contains eight Gell-Mann matrices of the 3rd rank $\lambda_1 - \lambda_8$ and the same number of Hubbard operators. Relations between the matrix of Hubbard operators and the Gell-Mann matrices for this group are also presented in Appendix. Further reduction of the energy interval $\mathcal{E} \ll \epsilon_i$ results in complete suppression of charged sectors $\mathcal{N} \neq 1$, so that we are left only with spin states $\sigma = \uparrow, \downarrow$. In this limit, the dynamical symmetry is the same as the symmetry of the Hubbard atom, and the corresponding Lie group is $SU(2)$.

Mathematically, nontrivial dynamical symmetries are described by semisimple groups, and the groups $SU(n)$ with $n > 2$ belong to this type of Lie groups. If the states in the Fock space for the Hubbard atom are ordered as

$$\bar{\Phi}_4 = (\uparrow \downarrow 0\ 2), \tag{3.5}$$

then the first three Gell-Mann matrices, λ_1–λ_3, are related to the spin states in the charge sector $\mathcal{N} = 1$. Next nine matrices, λ_4–λ_{12}, describe transitions between the adjacent charge sectors, $(\mathcal{N} = 1) \leftrightarrow (\mathcal{N} = 0,2)$, and the last three matrices, λ_{13}–λ_{15}, connect the charge sectors $\mathcal{N} = 0$ and $\mathcal{N} = 2$ (see Appendix).

It is expedient to rewrite the original Hamiltonian (3.3) in terms of the generators of the group $SU(4)$ in the case where all four eigenstates (3.4) shown in Fig. 1(a) are taken into account, and in terms of the $SU(3)$ generators in the case when the polar states with $\mathcal{N} = 2$ are frozen out [see Fig. 1(b)]. In the full space $\bar{\Phi}_4$, we obtain by means of Eq. (A2),

$$\hat{H}_d^{SU(4)} = \frac{E_0}{4}\left(1 - \frac{4}{\sqrt{3}}X_8\right) + \frac{E_1}{2}\left(1 + \frac{2}{\sqrt{3}}X_8 + \frac{2}{\sqrt{6}}X_{15}\right) + \frac{h}{2}X_3 + \frac{E_2}{4}(1 - \sqrt{6}X_{15}). \tag{3.6}$$

Here, the notation X_ρ is used for the Gell-Mann matrices λ_ρ defined in the Fock space (3.5). The Zeeman term hS_z acting in the charge sector $\mathcal{N} = 1$ is also added. In the reduced Fock subspace,

$$\bar{\Phi}_3 = (\uparrow \downarrow 0) \quad \text{or} \quad (\uparrow \downarrow 2), \tag{3.7}$$

the Hamiltonian of the Hubbard atom rewritten with the use of Eq. (A4) acquires a quite compact form:

$$\hat{H}_d^{SU(3)} = \frac{E_0}{3}(1 - \sqrt{3}X_8) + \frac{E_1}{3}(1 + \sqrt{3}X_8) + \frac{h}{2}X_3. \tag{3.8}$$

The Hubbard atom is a minimal model that can be used for the description of a quantum dot with variable occupation $\mathcal{N}$ coupled with the bath by means of the tunneling channel. The equilibrium occupation of the dot may be changed by means of injection of an electron or a hole from the metallic reservoir.[15] This occupation fluctuates dynamically due to the single electron tunneling (SET) between the dot and the leads. The Coulomb blockade parameter Q plays the same part as the Coulomb repulsion U in the original Hubbard model. In the general case of, say, planar quantum dot, the energy spectrum of a quantum dot contains many discrete states without definite angular symmetry. Only the highest occupied (HO) and the lowest unoccupied (LU) states are involved in single electron tunneling through such quantum dot. The Hamiltonian of subsystem $\mathcal{S}$ in the Hamiltonian (3.1) has the form

$$\hat{H}_d = \sum_j \varepsilon_j d_{j\sigma}^\dagger d_{j\sigma} + \hat{H}_{\rm int} + Q\left(n_{\rm dot} - \frac{v_g C_g}{e}\right)^2. \tag{3.9}$$

Here, the index j enumerates the levels bottom-up. $\hat{H}_{\rm int}$ is the electron-electron interaction in the quantum dot. Usually, the self-consistent Hartree term is included in the definition of discrete levels ε_j, and the relevant contribution to $\hat{H}_{\rm int}$ is the exchange between the electrons occupying different levels of a *neutral* quantum dot. $Q = e^2/2C$ is the capacitive energy of the dot, $n_{\rm dot} = \sum_{j\sigma}^{(\rm ext)} d_{j\sigma}^\dagger d_{j\sigma}$ is the number of *extra* electrons or holes that are injected in the dot due to tunneling described by the Hamiltonian $\hat{H}_{db}$,

$$\hat{H}_{db} = \sum_{l=s,d}\sum_{jk\sigma}(W_{lj} d_{j\sigma}^\dagger c_{lk\sigma} + \text{H.c.}). \tag{3.10}$$

Corrections to the capacitive energy take into account the capacitance of the gate C_g and the gate voltage v_g. If the

hierarchy of the energy scales

$$Q > (\delta\varepsilon, J) \gg W_{lj} \tag{3.11}$$

takes place ($\delta\varepsilon$ is the interlevel spacing between the HO and LU states, J is the exchange coupling constant), then one may assert that the charge transfer through the quantum dot occurs in the SET regime.

Variation of the energy spectrum and the occupation of the quantum dot as a function of a gate voltage is exemplified in Fig. 2. The "Hubbard parabolas"[30–33] represent the energy $E_{\rm el}(\mathcal{N})$ of the isolated quantum dot with the Hamiltonian (3.9). Three subsequent diagrams for the occupation $\mathcal{N}=1$ show the asymmetric configurations with quenched zero and two electron occupation (the side diagrams) and the configuration with particle-hole symmetry (the middle diagram). The single-particle excitations are the addition and extraction energies $E(\mathcal{N}) - E(\mathcal{N} \mp 1)$ that should be compared with the chemical potential of the bath (the Fermi energy)—see the lower panel of Fig. 2.

It is natural to rewrite the Anderson Hamiltonian in such a way that the addition energies appear explicitly in the zero-order terms (3.6) and (3.8). In order to do this, we express the Hubbard Hamiltonian (3.6) and the tunneling term H_{db},

$$H_{db} = \sum_{k\sigma} (t_k d^\dagger_{k\sigma} c_{k\sigma} + \text{H.c.}), \tag{3.12}$$

via the operators from the triads (A3), which are connected with the original Hubbard operators $X^{\Lambda\Lambda'}$ acting in the space (3.5) by the following relations:

$$\begin{aligned}
&\mathsf{T}^+ = X^{\uparrow\downarrow}, \quad \mathsf{T}^- = X^{\downarrow\uparrow}, \quad \mathsf{T}_z = X^{\uparrow\uparrow} - X^{\downarrow\downarrow},\\
&\mathsf{V}^+ = X^{\uparrow 0}, \quad \mathsf{V}^- = X^{0\uparrow}, \quad \mathsf{V}_z = X^{\uparrow\uparrow} - X^{00},\\
&\mathsf{U}^+ = X^{\downarrow 0}, \quad \mathsf{U}^- = X^{0\downarrow}, \quad \mathsf{U}_z = X^{\downarrow\downarrow} - X^{00},\\
&\mathsf{W}^+ = X^{\uparrow 2}, \quad \mathsf{W}^- = X^{2\uparrow}, \quad \mathsf{W}_z = X^{\uparrow\uparrow} - X^{22},\\
&\mathsf{Y}^+ = X^{\downarrow 2}, \quad \mathsf{Y}^- = X^{2\downarrow}, \quad \mathsf{Y}_z = X^{\downarrow\downarrow} - X^{22},\\
&\mathsf{Z}^+ = X^{02}, \quad \mathsf{Z}^- = X^{20}, \quad \mathsf{Z}_z = X^{00} - X^{22}.
\end{aligned} \tag{3.13}$$

Equations (3.13) realize the general expansion scheme (2.8) for the irreducible vector operators in the group $SU(4)$. The triad $\vec{\mathsf{T}}$ is nothing but the set of spin 1/2 operators $(S^+, S^-, 2S_z,)$ acting in the charge sector $\mathcal{N}=1$. The triad $\vec{\mathsf{Z}}$ describes the two-particle excitations ($\mathcal{N}=0 \leftrightarrow \mathcal{N}=2$) with the energy

$$E_{20} = E(\mathcal{N}=2) - E(\mathcal{N}=0). \tag{3.14}$$

The rest four triads describe ionization of the Hubbard atom with $\mathcal{N}=1$ addition and extraction energies

$$\begin{aligned}
E_{10} &= E(\mathcal{N}=1) - E(\mathcal{N}=0),\\
E_{12} &= E(\mathcal{N}=1) - E(\mathcal{N}=2).
\end{aligned} \tag{3.15}$$

These operators enter the Anderson Hamiltonian corresponding to the Hubbard parabolas of Fig. 2.

The Hamiltonian $\hat{H}_d^{SU(4)}$ may be expressed via the z components of irreducible vectors (3.13) by means of the following relations:

$$\begin{aligned}
\mathsf{Q}_z &= \mathsf{V}_\mathsf{z} + \mathsf{U}_\mathsf{z} = X^{11} - 2X^{00},\\
\mathsf{P}_z &= \mathsf{W}_\mathsf{z} + \mathsf{Y}_\mathsf{z} = X^{11} - 2X^{22},\\
2\mathsf{Z}_z &= \mathsf{Q}_z - \mathsf{P}_z = 2(X^{22} - X^{00})
\end{aligned} \tag{3.16}$$

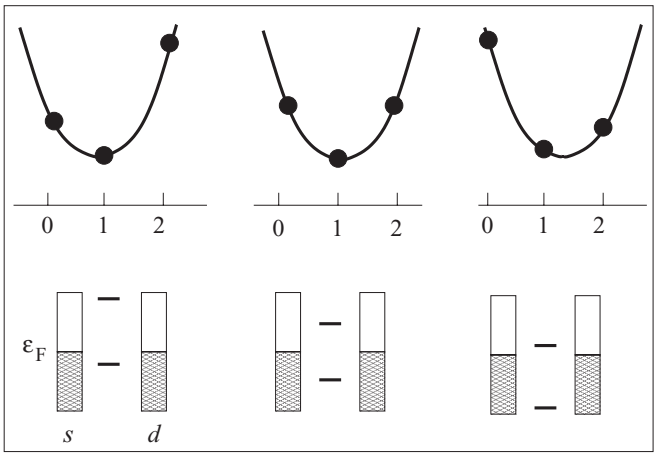

FIG. 2. (Upper panel) Variation of the energy of the quantum dot $E_{\rm el}(\mathcal{N})$ as a function of the gate voltage. (Lower panel) corresponding variation of addition energies for electron and hole excitations relative to the Fermi level in the leads. See the text for further discussion.

[see also Eq. (A5)]. The completeness condition (2.6) reads

$$X^{00} + X^{11} + X^{22} = 1, \quad X^{11} = \sum_\sigma X^{\sigma\sigma}. \tag{3.17}$$

We find from Eqs. (3.16) and (3.17) the following:

$$\begin{aligned}
&X^{00} = \tfrac{1}{4} - \tfrac{1}{8}(3\mathsf{Q}_z - \mathsf{P}_z), \quad X^{22} = \tfrac{1}{4} + \tfrac{1}{8}(\mathsf{Q}_z - 3\mathsf{P}_z),\\
&X^{11} = \tfrac{1}{2} + \tfrac{1}{4}(\mathsf{P}_z + \mathsf{Q}_z).
\end{aligned} \tag{3.18}$$

Using Eqs. (3.13), (3.16) and (3.17), we rewrite creation and annihilation operators as well as the occupation number operators for the dot electrons in terms of the Gell-Mann operators for $SU(4)$ group:

$$\begin{aligned}
&d^\dagger_\uparrow = \mathsf{V}^+ + \mathsf{Y}^-, \quad d^\dagger_\downarrow = \mathsf{U}^+ - \mathsf{W}^-,\\
&n_d = X^{\uparrow\uparrow} + X^{\downarrow\downarrow} + X^{22} = 1 + \tfrac{1}{2}(\mathsf{Q}_z - \mathsf{P}_z) = 1 + \mathsf{Z}_z.
\end{aligned} \tag{3.19}$$

Then the general $SU(4)$ configurations (the first and the third parabolas in Fig. 2) are described by the Hamiltonian

$$\begin{aligned}
\hat{H}^{SU(4)} = &\frac{2E_1 + E_0 + E_2}{4} \cdot \mathsf{G}_0 + \frac{h}{2} \cdot \mathsf{T}_z\\
&+ \frac{E_{10}}{4} \cdot \mathsf{Q}_z + \frac{E_{12}}{4} \cdot \mathsf{P}_\mathsf{z} + \frac{E_{20}}{4} \cdot \mathsf{Z}_z,
\end{aligned} \tag{3.20}$$

where G_0 is the unit Gell-Mann matrix in the Fock space Φ_4, $E_{ij} = E_i - E_j$ are the addition/extraction energies (3.14)/(3.15). Thus the operators $\mathsf{P}_z/4$, $\mathsf{Q}_z/4$, $\mathsf{Z}_z/4$, and $\mathsf{T}_z/2$ describe in the unified way all Fermi- and Bose-like excitations shown in Fig. 1(a). In the degenerate case $E_0 = E_2 \equiv E_e$ (second parabola in Fig. 2), this Hamiltonian reduces to

$$\hat{H}_d^{SU(4)} = \frac{E_1 + E_p}{2} \cdot \mathsf{G}_0 + \frac{h}{2} \cdot \mathsf{T}_z + \frac{E_{1e}}{4} \cdot (\mathsf{Q}_z + \mathsf{P}_z). \tag{3.21}$$

The tunneling term $\hat{H}_{db}$ also may be expressed via the generators of $SU(4)$ group, namely, via the ladder operators:

$$\hat{H}_{db}^{SU(4)} = \sum_k t_k (\mathsf{V}^\dagger + \mathsf{Y}^\dagger) c_{k\uparrow} + (\mathsf{U}^\dagger - \mathsf{W}^-) c_{k\downarrow} + \text{H.c.}. \tag{3.22}$$

In the strongly asymmetric situations (the side configurations in Fig. 2, where the excitation E_{01} is soft, whereas the excitation E_{21} is frozen out or vice versa), the symmetry of the dot is reduced from $SU(4)$ to $SU(3)$. Respectively, the system (3.18) reduces to

$$X^{00} = \frac{1}{3} - \frac{\mathsf{Q}_z}{3}, \quad X^{11} = \frac{2}{3} + \frac{\mathsf{Q}_z}{3}, \tag{3.23}$$

or, in terms of operators U,V,

$$X^{\uparrow\uparrow} = \frac{1}{3} + \frac{2\mathsf{V}_z - \mathsf{U}_z}{3}, \quad X^{\downarrow\downarrow} = \frac{1}{3} + \frac{2\mathsf{U}_z - \mathsf{V}_z}{3}. \tag{3.24}$$

The Anderson Hamiltonian acting in the space $\bar{\Phi}_3$ has the form

$$\hat{H}_d^{SU(3)} = \frac{2E_1 + E_0}{3} \cdot \mathsf{G}_0 + \frac{E_{10}}{3} \cdot (\mathsf{U}_z + \mathsf{V}_z) + \frac{h}{2} \cdot \mathsf{T}_z, \tag{3.25}$$

$$\hat{H}_{db}^{SU(3)} = \sum_k t_k[(\mathsf{V}^+ c_{k\uparrow} + \mathsf{U}^+ c_{k\downarrow}) + \text{H.c.}]. \tag{3.26}$$

Thus the operators describing the charge Hubbard excitations in the $SU(3)$ subspace $\bar{\Phi}_3$ (3.7) are $\vec{\mathsf{U}}$ and $\vec{\mathsf{V}}$, whereas the spin excitations are described by the conventional spin operator $\vec{\mathsf{S}} = \vec{\mathsf{T}}/2$.

The dynamics of charge and spin excitations in this case is predetermined by the commutation relations for the group generators. The operators O belonging to the same subgroup (triad) commute in accordance with the standard $SU(2)$ relations

$$[\mathsf{O}_z,\mathsf{O}^\pm] = \pm 2\mathsf{O}^\pm, [\mathsf{O}^+,\mathsf{O}^-] = \mathsf{O}_z. \tag{3.27}$$

The nonzero commutation relations between the operators belonging to different triads ensure complex dynamical properties of Hubbard-like SCES:

$$\begin{aligned} &[\mathsf{U}^\pm,\mathsf{V}^\mp] = \pm\mathsf{T}^\mp, \quad [\mathsf{U}^\pm,\mathsf{V}_z] = \mp\mathsf{U}^\pm, \\ &[\mathsf{U}_z,\mathsf{V}^\pm] = \pm\mathsf{V}^\pm, \quad [\mathsf{U}_z,\mathsf{V}_z] = 0. \end{aligned} \tag{3.28}$$

Respectively, the nonzero anticommutation relations are

$$\begin{aligned} \{\mathsf{U}^+,\mathsf{U}^-\} &= \frac{2 + \mathsf{V}_z - 2\mathsf{U}_z}{3}, \\ \{\mathsf{V}^+,\mathsf{V}^-\} &= \frac{2 + \mathsf{U}_z - 2\mathsf{V}_z}{3}. \end{aligned} \tag{3.29}$$

Then the excitations in the charge sector are described by the Green functions, which may be found directly from equations of motion for the generators of $SU(3)$ group,

$$G_v = \langle\langle \mathsf{V}^-(t)\mathsf{V}^+(0)\rangle\rangle, G_u = \langle\langle \mathsf{U}^-(t)\mathsf{U}^+(0)\rangle\rangle. \tag{3.30}$$

Respectively, the excitations in the spin sector are given by the Green functions

$$G_s = \langle\langle \mathsf{S}^-(t) \cdot \mathsf{S}^+(0)\rangle\rangle. \tag{3.31}$$

Here, the double brackets stand for thermal averaging and time-ordering operations specified for the retarded, advanced, or causal Green function. These functions can be easily found in the atomic limit where only the term $\hat{H}_d^{SU(3)}$ is retained. Solving equation of motion for the "Fermi-like" Green functions that describe excitations in the charge sector, one gets by means of the commutation and anticommutation relations (3.28) and (3.29):

$$\begin{aligned} G_v(\omega) &= \frac{i}{2\pi} \frac{(2 + \langle \mathsf{V}_z\rangle - 2\langle \mathsf{U}_z\rangle)/3}{\omega - \epsilon_d}, \\ G_u(\omega) &= \frac{i}{2\pi} \frac{(2 + \langle \mathsf{U}_z\rangle - 2\langle \mathsf{V}_z\rangle)/3}{\omega - \epsilon_d}. \end{aligned} \tag{3.32}$$

Using the definitions (3.23) and (3.24), we see that the numerators in the Green functions (3.32) are nothing but the averages $\langle X^{00}\rangle + \langle X^{\uparrow\uparrow}\rangle$ and $\langle X^{00}\rangle + \langle X^{\downarrow\downarrow}\rangle$, so that these functions are indeed the atomic Green functions for the Hubbard model[33] rewritten in terms of the generators of the $SU(3)$ group.

The "Bose-like" Green function G_s that describes the excitations in the spin sector in the atomic limit has the usual form

$$G_s = \frac{i}{2\pi} \frac{\langle \mathsf{S}_z\rangle}{\omega - h}. \tag{3.33}$$

To summarize the results obtained in this section, we stress once more that the dynamical symmetry of four-level system in the phase space $\bar{\Phi}_4$ (3.5) is indeed the local symmetry of the Anderson Hamiltonian, which allows the unified description of the evolution $SU(4) \to SU(3) \to SU(2)$ accompanying reduction of the energy scale $\mathcal{E}$ due to freezing of charge degrees of freedom (first partial then complete in accordance with Figs. 1 and 2). The phase space reduces appropriately $[\bar{\Phi}_4 \to \bar{\Phi}_3 \to \bar{\Phi}_2 = (\uparrow,\downarrow)]$. In all cases, the local Hamiltonian contains the z components of the group generators, and the perturbation includes the ladder operators. Respectively, the zero-order Green functions (3.32) and (3.33) describe the local excitations with the residues proportional to the averages of the same z components. Just these "bare" Green functions form the basis for various diagrammatic techniques elaborated for SCES.[47]

IV. IRREDUCIBLE REPRESENTATIONS FOR $SU(n)$ DYNAMICAL SYMMETRIES OF HUBBARD ATOM

As was noticed in the sixties,[4] various families of hadrons are classified in accordance with the irreducible representations of $SU(3)$ group (see also Ref. 48). In particular, 18 baryons form two multiplets corresponding to representations $D^{(11)}$ (the octet of baryons with spin 1/2) and $D^{(30)}$ (the decuplet of baryons with spin 3/2). The octet of spinless mesons also transforms along the representation $D^{(11)}$. The higher representations of the $SU(3)$ group are realized in the physics of strong interaction because these "composite" particles possess not only the spin and charge but also the isospin and hypercharge quantum numbers, and the $SU(3)$ symmetry characterizes the latter variables. The elementary particles obeying the $SU(3)$ symmetry are the colored quarks. The $SU(3)$ symmetry in the hadron multiplets under strong interaction is satisfied only approximately due to existence of electro-weak interaction, so that this symmetry may be treated as a dynamical symmetry in the original sense of this notion.

The Hubbard atom with frozen doubly occupied states possesses only two quantum numbers, namely, spin and

charge. Therefore the multiplet of Hubbard states is described by the lowest irreducible representation $D^{(10)}$ of the $SU(3)$ group. To construct this representation, one should recollect that the two of eight Gell-Mann matrices can be diagonalized simultaneously. Following Ref. 48 and basing on the Hamiltonian (3.25), we choose the representation with diagonal matrices $\mathsf{T}_z/2$ and $\mathsf{Q}_z/3$. Then the set of allowed states is defined by the two integer numbers λ,μ so that the eigenstates are determined as

$$M_T = \lambda + \mu, M_Q = \frac{\lambda - \mu}{3}. \tag{4.1}$$

The whole set of eigenstates form a two-dimensional triangular lattice on the plane (M_T, M_Q). Each irreducible representation $D^{\bar{\lambda}\bar{\mu}}$ is marked by the indices $\bar{\lambda},\bar{\mu}$ corresponding to the state with the maximum eigenvalue $\bar{M}_Q$ and the maximum value of $\bar{M}_T$ possible at this $\bar{M}_Q$. Then, the rest states forming this irreducible representation are constructed by means of the ladder operators $\mathsf{T}^{\pm},\mathsf{U}^{\pm},\mathsf{V}^{\pm}$ acting on the state $|\bar{M}_Q,\bar{M}_T\rangle$.

This procedure results in construction of the stars of basis vectors $\bar{D}^{\lambda\mu}$ and the polygons connecting the points generated by the ladder operators subsequently acting on the point $(\bar{M}_Q,\bar{M}_T)$. In the case of baryon family, the corresponding multiplets are the hexagon with doubly degenerate central point for representation $D^{(11)}$ and the triangle with ten point in its vertices and on its sides for representation $D^{(30)}$. In the case of Hubbard atom, the multiplet is represented by a triangle (see Fig. 3) labeled in accordance with the state with the highest quantum numbers $\lambda = 1,\mu = 0$, which corresponds to the state $|\mathcal{N},\sigma\rangle = |1,\uparrow\rangle$ of the Hubbard atom.

Two remaining components of the multiplet $\bar{\Phi}_3$ may be generated from the state $|1,\uparrow\rangle$ by means of the ladder operators $\mathsf{T}^- = X^{\downarrow\uparrow}$ and $\mathsf{V}^- = X^{0\uparrow}$. First of these operators corresponds to the "Bose-like" excitation with spin 1, and the second one is the "Fermi-like" excitation with spin 1/2. The triangle $D^{(10)}$ is closed by means of the operator $\mathsf{U}^+ = X^{\downarrow 0}$. The interrelations between the values of the parameters λ,μ, the eigenvalues M_T and M_Q of the operators $\mathsf{T}_z/2$ and $\mathsf{Q}_z/3$, and the eigenvalues $|\Lambda\rangle$ of the Hubbard Hamiltonian are presented in the following table:

λ	μ	M_T	M_Q	Λ
1	0	1/2	1/3	$\uparrow$
0	−1	−1/2	1/3	$\downarrow$
−1	1	0	−2/3	h

(4.2)

[see Eq. (A5)]. Here, the notation "h" is used for the hole state $|\Lambda\rangle = |0\rangle$.

Thus we see that the dual nature of the Hubbard operators manifested in the superalgebra with the commutation relations (2.7) allows one to use them for construction of the generic $SU(3)$ algebra formed by the operators with the commutation relations (3.27) and (3.28).

Like in the case of baryons and mesons, this symmetry is violated due to interaction with other subsystems. In our case, this is the Fermi bath $\mathcal{B}$. The source of this interaction is the tunneling coupling given by the Hamiltonian $\hat{H}_{db}^{SU(3)}$.

Generalization of this description for the $SU(4)$ group is straightforward. In this case, the phase space for the irreducible representations is defined by the eigenvalues of the operators P_z, Q_z, T_z, and the lowest irreducible representation of this group $D^{(100)}$ is represented by a triangular pyramid in this 3D space. Three indices of the representation $D^{(\lambda\mu\nu)}$ determine the eigenvalues M_T, M_Q, M_P of the operators $\mathsf{T}_z/2$, $\mathsf{Q}_z/4$, $\mathsf{P}_z/4$:

$$M_T = \frac{\lambda + \mu - \nu}{2}, \quad M_Q = \frac{\lambda - \mu + \nu}{4}, \quad M_P = \frac{\lambda - \mu - \nu}{4}. \tag{4.3}$$

The relations between the values of the parameters λ,μ,ν, the eigenvalues of the z components of the $SU(4)$ group generators and the eigenvalues $|\Lambda\rangle$ of the Hubbard Hamiltonian are summarized in the following table:

λ	μ	ν	M_T	M_Q	M_P	M_Z	Λ
1	0	0	1/2	1/4	1/4	0	$\uparrow$
0	−1	0	−1/2	1/4	1/4	0	$\downarrow$
−1	0	−1	0	−1/2	0	−1/4	h
0	1	1	0	0	−1/2	1/4	d

(4.4)

Here, "d" stands for $|\Lambda\rangle = |2\rangle$. The table includes also the eigenvalues $M_z = \nu/4$ of the operator $\mathsf{Z}_z/4$, which is the combination of two other operators, $M_z = (M_Q - M_P)/2$ [see Eq. (3.16)]. Due to above mentioned duality of $SU(4)$ group, the three eigenvalues M_Z, M_Q, M_P are involved in the negative-U model.

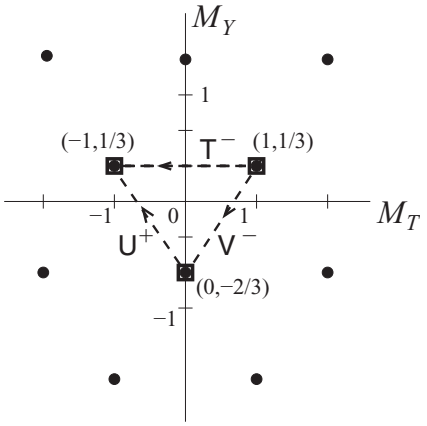

FIG. 3. Irreducible representation $D^{(10)}$ for the set $\bar{\Phi}_3$.

V. TWO-STAGE RENORMALIZATION GROUP FOR $SU(3)$ AND $SU(4)$ ANDERSON HAMILTONIAN

In this section, we will see how the hierarchy of dynamical symmetries of the Hubbard atom manifests itself in the RG evolution of the Anderson-Kondo problem. The RG method is based on the idea of renormalization of model parameters, which are relevant at low energy as a result of the change

of the scale of high-energy excitations.[22] If the model is renormalizable, any such parameter $P(\varepsilon)$ may be represented as

$$P(\varepsilon) - P[(1+\kappa)\varepsilon] = -\kappa\varepsilon P'(\varepsilon), \tag{5.1}$$

where κ is positive infinitesimal and the prime stands for the derivative. The quantity $-\kappa\varepsilon P'(\varepsilon)$ is the contribution to $P(\varepsilon)$ from the high-energy states, which are to be integrated out, preserving the form of $P(\varepsilon)$ but changing its scale.

Having in mind the definition of dynamical symmetry for correlated electrons presented in Sec. III, we see that the RG method is intimately related to the dynamical symmetries. First, the RG procedure reshuffles the energy states of the system $\mathcal{B}+S$, and second, in the process of renormalization, the energy scale reduces and this reduction results in successive freezing out high-energy states of subsystem $\mathcal{S}$, which, in turn, means reduction of dynamical symmetry of its energy spectrum. Adopting this approach, we immediately notice the inevitability of the three- or two-stage RG procedure as a direct consequence of several energy scales inherent in the Anderson model and the dynamical $SU(n)$ symmetry of its excitation spectrum with $n = 4$ or 3.

A. Model with Hubbard repulsion, $U > 0$

Taking as an example the first of three Hubbard parabolas in Fig. 2, we see that in this case the highest-energy scale is the addition energy $\mathcal{E} \sim \epsilon_d + Q - \varepsilon_F$. The corresponding generators of $SU(4)$ group are $\vec{\mathsf{W}}$ and $\vec{\mathsf{Y}}$. The next energy scale $\mathcal{E} \sim \varepsilon_F - \epsilon_d$ is the extraction energy, and the relevant generators are $\vec{\mathsf{U}}$ and $\vec{\mathsf{V}}$. The lowest-energy scale $\mathcal{E} \ll t^2/\epsilon_d$ is introduced by the second-order cotunneling processes from the dot to the leads, which are accompanied by the spin flips in the dot and creation of the low-energy electron-hole pairs in the leads. The vector operator $\vec{\mathsf{T}}$ is responsible for these processes. In other words, we arrive at the renowned Jefferson-Haldane-Anderson renormalization group (RG) procedure.[23,24] Basing on the symmetry analysis of preceding section, the RG procedure may be described in terms of the generators of $SU(4)$ group and its subgroups with the reduction of the symmetry $SU(4) \to SU(3) \to SU(2)$ following the reduction of the energy scale $\mathcal{E}$.

Instead of renormalization of the energy levels E_Λ used in the original "poor man's" theory,[24] we may use the advantages of the Gell-Mann representation and turn directly to renormalization of excitations entering the denominators of the Green's functions. Let us rederive, for example, the scaling equations for the two stage RG $SU(3) \to SU(2)$ realized in the limit $U \to \infty$ in these new terms. In the Anderson model, the change of the energy scale in Eq. (5.1) means the contraction of the electron bandwidth $D \to D - \delta D$ in $\hat{H}_b$. The renormalized quantities are the self-energies $\Sigma_\eta(\varepsilon)$ of the Green functions (3.30) and (3.31), $\eta = u,v,s$. The tunneling Hamiltonian (3.26) gives the second-order self-energy part for the Green functions G_v, G_u (3.32),

$$\epsilon_d = E_{10} + \frac{\Gamma}{\pi}\int_0^D \frac{d\varepsilon}{E_{10}-\varepsilon}, \tag{5.2}$$

where

$$\Gamma = \Gamma_u = \Gamma_v = \pi\sum_k |t_k|^2\delta(\varepsilon_F - \varepsilon_k)$$

is the spin-independent tunneling rate. The transformation (5.1) applied to Eq. (5.2) results in the Jefferson-Haldane scaling equation[23,24]

$$\frac{d\epsilon_d}{dD} = \frac{\Gamma}{\pi D} \tag{5.3}$$

with the scaling invariant

$$\epsilon_d^* = \epsilon_d + \frac{\Gamma}{\pi}\ln\left(\frac{\pi D}{\Gamma}\right). \tag{5.4}$$

Thus the evolution of the resonance level is determined by the vectors $\vec{\mathsf{U}}$ and $\vec{\mathsf{V}}$ operating in the charge subsectors of the group $SU(3)$. The same second-order processes generate the four-tail vertices $\sim \mathsf{V}^+\mathsf{U}^- c^\dagger_{k\downarrow}c_{k'\uparrow}$, $\mathsf{U}^+\mathsf{V}^- c^\dagger_{k\uparrow}c_{k'\downarrow}$, etc. Using the commutation relations (3.28), these vertices are combined in the conventional Schrieffer-Wolff exchange interaction

$$H_{\mathrm{SW}} = J\vec{\mathsf{S}}\cdot\vec{\mathsf{s}}, \tag{5.5}$$

where $\vec{\mathsf{s}} = N^{-1}\sum_{kk'} c^\dagger_{k'\sigma}\hat{\tau}c_{k'\sigma'}$ is the local spin operator for conduction electrons, $\hat{\tau}$ is the the vector of Pauli matrices, and $J| \sim t_{k_F}|^2/E_{10}$ is the indirect Kondo exchange. The scaling equations for this Hamiltonian may be derived by means of the Anderson's RG procedure.

In the symmetric configuration (middle parabola in Fig. 2), the Jefferson-Haldane-Anderson scaling theory is in fact the manifestation of reduction of the dynamical symmetry $SU(4) \to SU(2)$ in which the charge excitations represented by the vectors $(\vec{\mathsf{W}},\vec{\mathsf{Y}},\vec{\mathsf{U}},\vec{\mathsf{V}})$ are frozen out in the process of renormalization and the subgroup $\vec{\mathsf{T}}$ describing the spin degrees of freedom in the charge sector $\mathcal{N} = 1$ represents the low-energy part of the spectrum responsible for the Kondo singularities. Five vectors of six triads available in the Gell-Mann set are involved in this two-stage procedure.

B. Model with Hubbard attraction, $U' < 0$

Another choice of 15 linearly independent generators of the $SU(4)$ dynamical symmetry is possible in the case where instead of the spin degeneracy of the ground state with $\mathcal{N} = 1$ the charge degeneracy of the two singlets with $\mathcal{N} = 0,2$ is realized. Such a possibility arises in the negative U Anderson model.[27,28,49] In this configuration, the vector $\vec{\mathsf{T}}$ is excluded from the renormalization procedure due to quenching of the sector $\mathcal{N} = 1$ at low energies. Instead, the vector $\vec{\mathsf{Z}}$ is involved in formation of the Kondo singularities. The attractive interaction between the electrons in the nano-object in this model stems from the strong electron-phonon interaction. Starting with the Anderson-Holstein model where the phonon subsystem is represented by the single Einstein mode with the energy Ω_0, one may perform the canonical transformation,[50] which transforms the electron-phonon interaction into the polaron dressing exponent for the electron tunneling rate, the polaron shift of discrete electron levels and the phonon mediated electron-electron interaction. The latter renormalizes

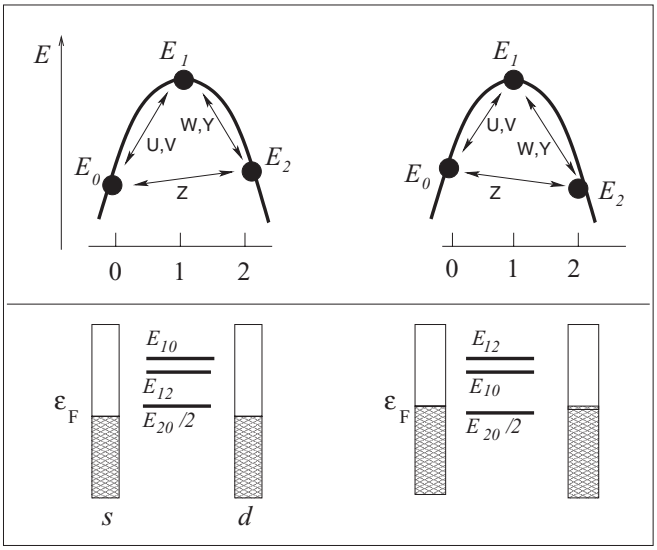

FIG. 4. (Upper panel) inverted Hubbard parabolas for the negative U Hubbard atom in the cases of empty and doubly occupied shells. The interlevel transitions are described by the operators generating the $SU(4)$ dynamical group. (Lower panel) single-electron levels corresponding to the transitions shown by the arrows in the upper panel (see the text for further explanation).

the Hubbard interaction term in the Anderson Hamiltonian:

$$U' = U - 2\lambda^2\Omega_0. \tag{5.6}$$

Here, λ is the electron-phonon coupling constant. In the limit of strong electron-phonon coupling, the energy gain due to the phonon mediated interaction overcomes the energy loss due to the Hubbard repulsion, and one comes to the case $U' < 0$. The negative U model may be realized in the single electron molecular transistors.[51–56] The interaction (5.6) should be included in the term $\hat{H}_d$, so that in the negative U case, the Hubbard parabolas for the energy spectrum are reversed relative to the usual shape shown in the middle configuration of Fig. 2. The "turned over" diagrams corresponding to the two nearly symmetric configurations shown in Fig. 4.

Like in the positive U case, the transitions between the levels in the Hubbard supermultiplet are described by the operators (3.13) generating the $SU(4)$ dynamical symmetry group. We consider here the configurations, where the singlet states $|\Lambda\rangle = |0\rangle,|2\rangle$ are degenerate or nearly degenerate, and the spin doublet $|\Lambda\rangle = |\uparrow\rangle,|\downarrow\rangle$ is an excited virtual state in the cotunneling processes. The two configurations presented in Fig. 4 correspond to the empty and completely filled two-electron shell of the Hubbard atom. They are connected by the particle-hole symmetry transformation, so it is enough to discuss one of them.

We will show below that the negative U Anderson model may be formally mapped on the positive U model, by means of the multistage RG method, which generalizes the Jefferson-Haldane-Anderson procedure[20,23,24] mentioned above. In the positive U case, after freezing out the high-energy excitations E_{01} and E_{21} corresponding to injection of a hole or of an electron into the singly occupied quantum dot at the Jefferson-Haldane stage of the renormalization, one arrives at the Anderson stage of Kondo screening of spin excitations in the sector $\mathcal{N} = 1$ described by the vector operator $\vec{\mathsf{T}}$. In the negative U model, the spin excitations are exponentially suppressed from the very beginning. After freezing out the charge excitations E_{10} and E_{12} generated by the operators $\vec{\mathsf{U}},\vec{\mathsf{V}},\vec{\mathsf{W}},\vec{\mathsf{Y}}$, we are left only with the two-particle charge excitations E_{20} generated by the operator $\vec{\mathsf{Z}}$.

Since the Jefferson-Haldane stage of the RG procedure is realized exactly in the same way as in the positive U Anderson model, we concentrate on the second stage, where the $SU(4)$ dynamical symmetry group is reduced to its $SU(2)$ subgroup represented by the triad $\vec{\mathsf{Z}}$. These operators act in the subspace $\bar{\Phi}_2 = (0,2)$. The effective SW Hamiltonian in this subspace reads

$$\hat{H}_{\text{cotun}} = N\frac{J_\perp}{2}(\mathsf{Z}^+\mathsf{B}^- + \mathsf{Z}^-\mathsf{B}^+) + NJ_\parallel \mathsf{Z}_z\mathsf{B}_z, \tag{5.7}$$

where the components of the vector $\vec{\mathsf{Z}}$ are presented in the last line of the system (3.13). The components of the vector $\vec{\mathsf{B}}$ defined in the space of two-particle itinerant excitations are

$$\mathsf{B}^+ = N^{-1}\sum_{kk'} c^\dagger_{k\uparrow}c^\dagger_{k'\downarrow}, \quad \mathsf{B}^- = N^{-1}\sum_{kk'} c_{k\downarrow}c_{k'\uparrow},$$
$$\mathsf{B}_z = N^{-1}\sum_{kk'}(c^\dagger_{k\uparrow}c_{k'\uparrow} - c_{k'\downarrow}c^\dagger_{k\downarrow}) = N^{-1}\sum_{kk'}\sum_{\sigma} c^\dagger_{k\sigma}c_{k'\sigma} - 1. \tag{5.8}$$

These operators obey the $SU(2)$ commutation relations

$$[\mathsf{B}^+,\mathsf{B}^-] = \mathsf{B}_z, [\mathsf{B}_z,\mathsf{B}^\pm] = \pm 2\mathsf{B}^\pm. \tag{5.9}$$

The transversal part of the Hamiltonian (5.7) describes the tunneling of singlet electron pairs between the leads and the molecule, whereas its longitudinal part stems from the band electron scattering on the charge fluctuations.

Thus the Hamiltonian of two-electron tunneling is formally mapped onto the anisotropic Kondo Hamiltonian[27,28,51] (see Fig. 5). The origin of this anisotropy is the polaron dressing of

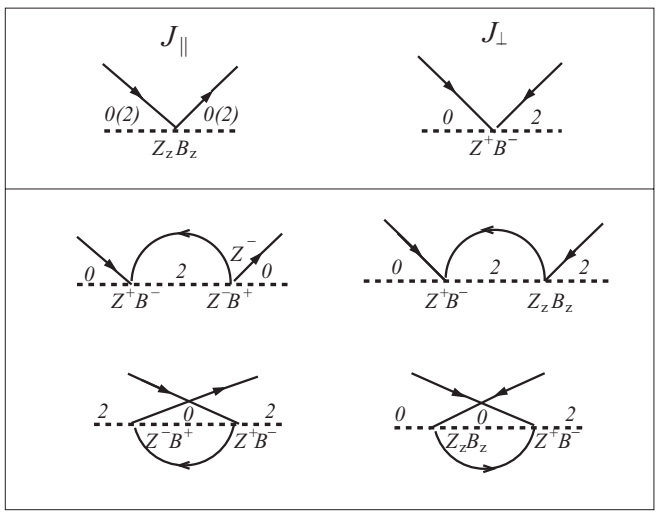

FIG. 5. RG diagrams in the space $\bar{\Phi}_2 = (0,2)$. (Upper panel) the bare vertices $J_\perp$ for the two-electron tunneling and $J_\parallel$ for the charge scattering. (Lower panel) the diagrams for the second-order renormalization of these vertices. Solid lines stand for the conduction electron states, dashed lines denote the charge states of the molecule.

tunneling matrix elements.[51] This dressing is different for the two-electron cotunneling and the electron scattering coupling parameters in the Hamiltonian (5.7). In the strong electron-phonon coupling limit, $(\lambda/\Omega_0)^2 = S \gg 1$,

$$\frac{J_\perp}{J_\parallel} = \langle 2|0\rangle \sim e^{-2(\lambda/\Omega_0)^2}. \tag{5.10}$$

The eventual source of this anisotropy is the overlap between the phonon wave functions for a molecule in the charge states $\mathcal{N} = 0$ and 2, i.e., the Huang-Rhys factor S.

In a framework of the Anderson RG scaling procedure, this means that the renormalization diagrams for the two models are the same, namely, the diagrams in the first and the second columns of Fig. 5 are mapped on the longitudinal and transversal components of the Kondo exchange Hamiltonian (5.5). The mapping procedure implies the substitution $\vec{\mathsf{S}} \to \vec{\mathsf{Z}}$, $\vec{\mathsf{s}} \to \vec{\mathsf{B}}$. The scaling equations, which follow from these equations are the same as for the conventional anisotropic Kondo model,[20] namely,

$$\frac{dj_\parallel}{d\eta} = -j_\perp^2, \quad \frac{dj_\perp}{d\eta} = -j_\perp j_\parallel \tag{5.11}$$

($j_i = \rho_0 J_i$). In the case of strong anisotropy (5.10), the solution of this system gives for the Kondo temperature the following equation:[51]

$$T_K \sim \left(\frac{j_\perp}{j_\parallel}\right)^{1/j_\parallel} \sim \bar{D}\exp\left[-\frac{\pi\Omega_0}{2\Gamma}\left(\frac{\lambda}{\Omega_0}\right)^4\right]. \tag{5.12}$$

The last equation in (5.12) is valid in the limit of strong electron-phonon coupling $S \gg 1$. Generally, the polaron narrowing of the tunneling rate results in a noticeable decrease of T_K in comparison with its value for the conventional Kondo effect.

We have demonstrated in this section that the dynamical symmetry is the same for the negative and positive U Anderson models. However, in spite of the formal similarity between the effective Hamiltonians for the single electron cotunneling and the electron pair cotunneling, the background physics is different in two versions of the Anderson model. In the positive U Anderson model, the tunneling in the middle of the Coulomb window arises exclusively due to the many-body Abrikosov-Suhl resonance. In the negative U model, the resonance conditions for the two-electron tunneling arise at $E_{02} = 0$ irrelatively to the many body particle-hole screening mechanism, so that the zero bias anomaly in the tunneling conductance exists already at $T \gg T_K$ as well as the finite bias anomaly at $E_{02} \neq 0$.[54–56] One may say that the Anderson orthogonality catastrophe[40] responsible for the many-body Kondo-like screening at low T only enhances the two-electron tunneling resonance already sharpened due to nonorthogonality of the phonon clouds measured by the Huang-Rhys factor (5.10). The finite difference $E_{02} \neq 0$ in the negative U model is equivalent to the finite magnetic field in the positive U model: it results in the appearance of two split finite bias peaks in the tunneling conductance.

Having in mind all these differences, one may state that the multistage RG procedure reveals the hierarchy of reduced dynamical symmetries $SU(4) \to SU(3) \to SU(2)$ in the Anderson model both with the Hubbard repulsion for odd occupation and with the Hubbard attraction for even occupation.

VI. MIXED-VALENCE REGIME

Let us apply the $SU(n)$ symmetry analysis to the mixed valence (MV) regime where in accordance with Haldane's classification,[24] the scaling invariant of the RG theory (5.4) satisfies the condition $|\epsilon_d^* - \varepsilon_F| \lesssim \Gamma$. The MV regime is the basic configuration, where the $SU(4)$ symmetry is a genuine symmetry of the ground state $|\Phi_0\rangle$ and the excitations $|\Psi_e\rangle$ related to the "impurity" center. This means that the interlevel transitions shown in Fig. 1 are involved in formation of $|\Phi_0\rangle$ and $|\Psi_e\rangle$ both in the weak and the strong coupling regimes.[25,26]

Indeed, in the trivial case of $U = 0, \epsilon_d - \varepsilon_F < 0$, we start with the doubly occupied dot, $\mathcal{N} = 2$, and completely filled Fermi sphere of the reservoir, so that the actual interlevel transitions are $E_{21} = E_{2\uparrow} = E_{2\downarrow} = \epsilon_d - \varepsilon_F$. The ground state of the system is spin singlet due to the Pauli principle, and the structure of the spectrum is described in terms of Friedel resonances for two spin projections. The wave functions of the excitations with extra electron may be found exactly:

$$\begin{aligned} |\Psi_\uparrow\rangle &= D^{-1/2}\left[(\mathsf{V}^+ + \mathsf{Y}^-) + \sum_k A_k c_{k\uparrow}^\dagger\right]|\Phi_0\rangle, \\ |\Psi_\downarrow\rangle &= D^{-1/2}\left[(\mathsf{U}^+ - \mathsf{W}^-) + \sum_k A_k c_{k\downarrow}^\dagger\right]|\Phi_0\rangle \end{aligned} \tag{6.1}$$

(D is the normalization factor). At finite U, the excitation spectrum may be found as a result of diagonalization of the scattering S matrix by means of the Bethe ansatz procedure. The elements of this matrix are determined by the Schroedinger equation for the two electron singlet states with the eigenvector,[25] which can be rewritten in terms of the generators of $SU(4)$ group:

$$\begin{aligned} |\Psi\rangle = \Big\{ &\int dx_1 dx_2 A(x_1,x_2) c_\uparrow^\dagger(x_1) c_\downarrow^\dagger(x_2) \\ &+ \int dx\, B(x)[c_\uparrow^\dagger(x)(\mathsf{U}^+ - \mathsf{W}^-) \\ &- c_\downarrow^\dagger(x)(\mathsf{V}^+ + \mathsf{Y}^+)] + C\mathsf{Z}^-\Big\}|0\rangle, \end{aligned} \tag{6.2}$$

so that the ladder generators of $SU(4)$ group are involved. Here, the vacuum state is defined as an empty dot and the filled Fermi sphere.

Of course, these excitations are complex many-body states. According to the exact solution, local charge excitations (holons) are singlet $2e$ holes dressed by the electron back-flow, so that the effective charge of spinless holon is e. Respectively, spinons are complex excitation where a spinful electron is dressed by the back-flow, which exactly compensates its charge but leaves intact its spin.[26] In the mixed valence regime, the spectral densities of charge and spin excitations are centered around zero and strongly overlapped, while in the Kondo regime, the spinon and holon spectra are separated from each other by the energy gap. The ladder operators from the triad T formally do not enter expansion (6.2) but in fact they are involved in formation of the many-particle ground state and

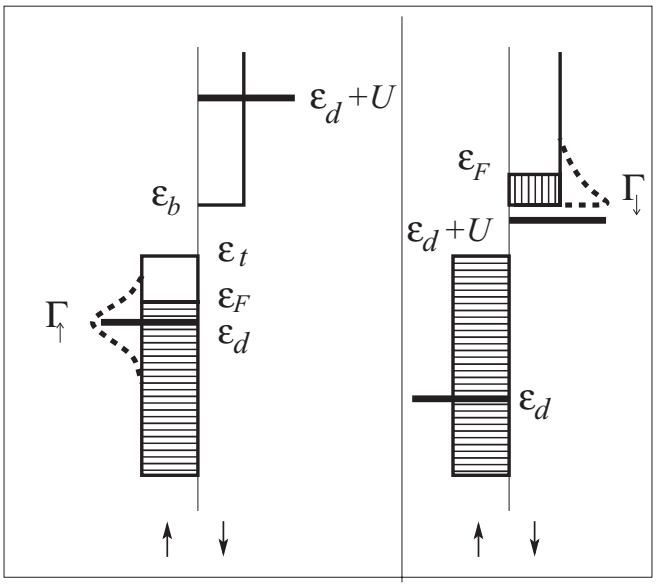

FIG. 6. (Left) Energy level scheme for quantum dot with occupation $\mathcal{N}=1$ in a contact with fully spin polarized metallic leads. (Right) The same for $\mathcal{N}=2$.

low-energy excitations via the higher ordering rescattering processes due to the commutation relations (3.28).

In situations, where the spin-flip excitations described by the vector T are frozen at low energies for some physical reason, the mixed-valence state involves only the operators $\mathsf{U},\mathsf{V},\mathsf{W},\mathsf{Y}$ from the charged sector. An example of such situations is a quantum dot in a tunneling contact with half-metallic (fully spin-polarized) leads (see Fig. 6).

In these systems, the gap for the spin-flip processes exists in the ferromagnetic leads due to full polarization of conduction electrons. The molecular field in the leads induces "stray" magnetic field in the dot due to mutual interpenetration of the wave functions (tunneling hybridization t_k in the Hamiltonian $\hat{H}_{db}$, see, e.g., Ref. 57). This field, in turn, polarizes the dot. As a result, at large enough U, the level ϵ_d occupied by spin up electron is hybridized with majority spin in the band $\epsilon_{k\uparrow}$, whereas the empty level ϵ_d+U is hybridized with the empty band $\epsilon_{k\downarrow}$, and the spin-flip processes are strongly suppressed at energies $\omega \lesssim \Gamma$. Due to this suppression, the excitations described by the vectors U and V are not interlaced. Then, in accordance with the RG approach, the low-energy properties of the system are determined by the energy scale $E\sim\varepsilon_t-\varepsilon_d$, and the Dyson equation for the excitations in the V sector may be solved exactly. The result for the dot Green functions is

$$G_v(\omega)=\frac{i}{2\pi}\frac{(2+\langle \mathsf{V}_z\rangle-2\langle \mathsf{U}_z\rangle)/3}{\omega-E_{10}-\Sigma_v(\omega)}, \tag{6.3}$$

where

$$\Sigma_v(\omega)=\frac{\Gamma_\uparrow}{\pi}\int^{\varepsilon_t}\frac{d\varepsilon}{\omega-\varepsilon} \tag{6.4}$$

[cf. (5.2)]. Here, the real and imaginary parts of the self energy $\Sigma_v(\omega)$ describe the Friedel shift and damping of the resonance level $E_{10}\to\varepsilon_d+i\Gamma_\uparrow$ (see the left panel of Fig. 6). We see that the dot states retain their $SU(3)$ symmetry.

Even more fundamental statement may be formulated in the case, where the renormalized level shifts to the energy gap[58,59] (see Fig. 6, right panel). In this case, corresponding to the charge sector $\mathcal{N}=2$ the canonical transformation for the discrete states may be offered:[60,61]

$$\widetilde{\mathsf{W}}^-=\mathsf{W}^-\cos\gamma_\downarrow+C^\dagger_\downarrow K_w\frac{\sin\gamma_\downarrow}{\gamma_\downarrow} \tag{6.5}$$

with

$$C^\dagger_\sigma=\sum_k c^\dagger_{k\sigma},\quad K_w=\frac{2+\mathsf{W}_z-2\mathsf{Y}_z}{3}. \tag{6.6}$$

The coefficients in this transformation are predetermined by the energy dependence of the self-energy

$$\Sigma_w(\omega)=\frac{\Gamma_\downarrow}{\pi}\int_{\varepsilon_b}\frac{d\varepsilon}{E_{21}-\varepsilon} \tag{6.7}$$

in the discrete part of the spectrum,

$$\tan^2\gamma_\downarrow=-\frac{d\Sigma_w(\omega)}{d\omega}\bigg|_{\omega=\varepsilon_\downarrow}. \tag{6.8}$$

The position of the renormalized level $\varepsilon_{d\downarrow}=\widetilde{E}_{12}$ in the energy gap is determined by the integral equation

$$\widetilde{\varepsilon}_{d\downarrow}=\varepsilon_d+\widetilde{U}+\Sigma_w(\varepsilon_{d\downarrow}). \tag{6.9}$$

Not only the "atomic" energy level is renormalized in Eq. (6.9), but also the Coulomb repulsion is reduced due to charge transfer between the dot and the leads, $U\to\widetilde{U}$. Due to the same charge transfer the actual occupation of dot is $n_d<2$ (see Fig. 6, right panel) and $n_d<1$ (see Fig. 6, left panel) provided the level width $\Gamma_\downarrow>\varepsilon_F-\varepsilon_b$ and $\Gamma_\uparrow>\varepsilon_F-\varepsilon_d$, respectively.

The last example of mixed valence solution in a half-metal with discrete level $\widetilde{\varepsilon}_{d\downarrow}$, where the Kondo correlations are completely suppressed, demonstrate especially distinctly that the $SU(3)$ symmetry is indeed the intrinsic symmetry of the Anderson model. As a result of tunneling (or hybridization) charge transfer between the dot (or impurity), a sort of "pseudoatom" arises, where the dot electron wave functions are extended into the regions where itinerant electrons reside, but the basic $SU(3)$ symmetry of the Hamiltonian $\hat{H}_d$ remained unperturbed as a result of transformation (6.5).

VII. $SU(4)$ DYNAMICAL SYMMETRY FOR THE HUBBARD LATTICE

As is known,[29,62,63] the eigenstates of the Hubbard model on a bipartite lattice may be classified along the representations of the $SO(4)$ group. It is instructive to trace how this global symmetry of the Hubbard lattice is related to the local $SU(4)$ dynamical symmetry of a Hubbard atom with the Hamiltonian $\hat{H}_{dm}$ on a site m. We will discuss this correlation by the example of the integrable Hubbard chain model with the Hamiltonian

$$\hat{H}_{\rm Hub}=\sum_{m=1}^{L}(\hat{H}_{dm}+td^\dagger_{m\sigma}d_{m+1}) \tag{7.1}$$

under conditions of particle-hole symmetry, $\epsilon_d-\varepsilon_F=U/2$ (central column in Fig. 2). Here, the number of sites L in the chain is even and the cyclic boundary conditions $L+1=1$ are adopted.

One may find the Casimir operator commuting with all generators of $SU(4)$ group (3.13) acting at each site m, namely,

$$\mathcal{C}_m = \vec{\mathsf{T}}_m^2 + \vec{\mathsf{U}}_m^2 + \vec{\mathsf{V}}_m^2 + \vec{\mathsf{W}}_m^2 + \vec{\mathsf{Y}}_m^2 + \vec{\mathsf{Z}}_m^2 = \frac{9}{2}\mathsf{G}_0. \quad (7.2)$$

Each term in this sum as well as the operators P_z, Q_z, T_z commute with the Hamiltonian $\hat{H}_{dm}$. Two operators commuting with the Hubbard Hamiltonian on a bipartite lattice may be introduced. These are the operators of the full spin and the η spin, generating $SU(2)$ spin and $SU(2)$ charge subgroups of the semisimple group $SO(4) \to SU(2) \times SU(2)/Z_2$. Both these operators may be expressed in terms of the generators of local $SU(4)$ symmetry. In case of the 1D Hubbard chain, these expressions read

$$\mathsf{S}^\alpha = \sum_{m=1}^{L} d^\dagger_{m\sigma}\tau^\alpha_{\sigma\sigma'}d_{m\sigma'} = \frac{1}{2}\sum_{m=1}^{L}\mathsf{T}^\alpha_m \quad (7.3)$$

($\alpha = \pm, z$, τ^α are the corresponding Pauli matrices),

$$\eta^+ = \sum_{m=1}^{L}(-1)^{m+1}d^\dagger_{m\uparrow}d^\dagger_{m\downarrow} = \sum_{m=1}^{L}(-1)^{m+1}\mathsf{Z}^+_m,$$
$$\eta^- = \sum_{m=1}^{L}(-1)^{m+1}d_{m\downarrow}d_{m\uparrow} = \sum_{m=1}^{L}(-1)^{m+1}\mathsf{Z}^-_m, \quad (7.4)$$
$$\eta^z = \sum_{m=1}^{L}(n_{m\uparrow} + n_{m\downarrow} - 1) = \frac{1}{2}\sum_{m=1}^{L}\mathsf{Z}^z_m.$$

The group generators $\vec{\mathsf{S}}$ and $\vec{\eta}$ act in the subspaces $\{\uparrow,\downarrow\}$ and $\{0,2\}$ of the full Fock space, respectively. They commute with the Hubbard chain Hamiltonian and form two Casimir operators $\vec{\mathsf{S}}^{\,2}$ and $\vec{\eta}^{\,2}$. The operators belonging to each of two triades $\vec{\mathsf{S}}$ and $\vec{\eta}$ obey the Pauli-like commutation relations, and $[\mathsf{S}^\alpha, \eta^\beta] = 0$.

This spin-charge separation of the variables, is characteristic also for the excitation spectrum. In particular, the Bethe ansatz solution of the problem uses the set of states with N electrons and M down spins. This solution may be constructed by means of the well defined procedure using the operators (7.3) and (7.4), which act on the state $|\psi_{k,\lambda}\rangle$ with given charge momentum k, spin rapidity λ and the highest weight of the total spin, so that $\mathsf{S}^+|\psi_{k,\lambda}\rangle = 0$, $\mathsf{S}^z|\psi_{k,\lambda}\rangle = \frac{1}{2}(N - 2M)|\psi_{k,\lambda}\rangle$ (cf. the choice of the state $|\bar{M}_Q, \bar{M}_T\rangle$ in the previous section). The set of regular Bethe ansatz states has the following structure:

$$|\psi_{k,\lambda,\alpha,\beta}\rangle = (\zeta^\dagger)^\alpha(\eta^\dagger)^\beta|\psi_{k,\lambda}\rangle. \quad (7.5)$$

Here, the vector $\vec{\zeta}$ with the components $\zeta^\mp = \mathsf{S}^\pm$, $\zeta^z = -\mathsf{S}^z$ is the contravariant partner of the vector $\vec{\mathsf{S}}$.

Thus we see that the excitation spectrum of the Hubbard chain may be constructed by means of the generators of local dynamical $SU(4)$ symmetry of the Hubbard atom. Apparently, this statement is valid in a more general context; for example, the Ward identities connecting the vertex functions and the Green functions on a bipartite Hubbard lattice[63] are derived by means of the same generators $\vec{S}$ and $\vec{\eta}$.

The last example reflects the duality of the triads $\vec{\mathsf{S}}$ and $\vec{\mathsf{Z}}$, which was mentioned above. Due to this immanent duality of $SU(4)$ operators acting in Φ_4, the negative U Hubbard model may be treated by means of the same tools as the positive U model similarly to the Anderson Hamiltonian.

VIII. CONCLUDING REMARKS

In this paper, we have shown that the "atomic" part $\hat{H}_d$ of the Anderson and Hubbard Hamiltonians may be treated as a four-level system in the mixed charge-spin space Φ_4 (3.5), so that the interlevel transitions induced by the tunneling term $\hat{H}_{db}$ activate the implicit $SU(4)$ dynamical symmetry of the model. In many cases, this symmetry is manifested only at high energies, whereas at low energies, only one or two subgroups of the full $SU(4)$ group survive in the low-energy part of excitation spectra. The form of the Hamiltonian $\hat{H}_d$ (3.21), (3.25) demonstrates explicitly that the Gell-Mann matrices of the 4th and 3rd rank provide the natural tool for treating the excitations in the Fock spaces Φ_4 and Φ_3, respectively. The Casimir operator for the group $SU(4)$ is given by Eq. (7.2), so that neither the local spin, nor the local charge of a "Hubbard atom" are good quantum numbers in the general case of an interacting system $\mathcal{S} + \mathcal{B}$. One may say that the basic properties of SCES described by the Hubbard and Anderson Hamiltonians are characterized not only by the conventional symmetry of these Hamiltonians but also by the dynamical symmetry of excitation spectra.

The Gell-Mann representation for SCES with zero-order Hamiltonian $\hat{H}_d$ (3.2) transformed into Eq. (3.21) or (3.25) allows one to describe directly the excitation spectra in charge and spin sectors within the unified formalism based on calculations of the self-energy diagrams for the renormalized Green functions (3.32) and (3.33). Of course, the non-Abelian Gell-Mann algebras like (3.27) and (3.28) make difficult any practical calculations based on the Feynman diagrammatics that appeals to the Wick's theorem (see, e.g., Ref. 47). In order to restore simple Feynman rules, various bosonization and fermionization procedures for the generators (3.13) may be chosen.[64–67] For example, the slave boson factorization for the group $SU(3)$ reads

$$\mathsf{V}^+ = f^\dagger_\uparrow h, \quad \mathsf{V}^- = f_\uparrow h^\dagger, \quad \mathsf{V}_z = f^\dagger_\uparrow f_\uparrow - h^\dagger h,$$
$$\mathsf{U}^+ = f^\dagger_\downarrow h, \quad \mathsf{U}^- = f_\downarrow h^\dagger, \quad \mathsf{U}_z = f^\dagger_\downarrow f_\downarrow - h^\dagger h, \quad (8.1)$$
$$\mathsf{T}^\alpha_{\sigma\sigma'} = f^\dagger_\sigma \tau^\alpha_{\sigma\sigma'} f_{\sigma'} h h^\dagger,$$

where $f^\dagger_\sigma$ and $h^\dagger$ are chargeless spin-fermion operators and spinless boson (holon) operators, respectively. The toll for this factorization is the necessity to project out the nonphysical states with zero and two fermions. The vertices also become more complicated. In particular, the two-tail vertices in the tunneling Hamiltonian (3.26) transform into the three-tail vertices $\sim f^\dagger_\sigma h c_{k\sigma}$. Then the temptation arises to introduce the mean field decoupling $\sim\langle h\rangle f^\dagger_\sigma c_{k\sigma}$ or, at least, to consider spin fermion and holon as two independent dynamical variables. It was noticed[68] that such decoupling violates the gauge invariance $U(1)$ of the Hamiltonian. In order to restore this invariance, one has to ascribe a charge gauge phase to chargeless spin fermions. We conclude from above consideration that such decoupling also violates the $SU(3)$ symmetry of the Anderson and Hubbard models. In particular, it is seen from the structure of the zero-order Hamiltonian $\hat{H}_d$ that E_{10} is the eigenstate of the operator Q_z, which fixes not the holon and

spin-fermion occupation numbers but their difference

$$\mathsf{V}_z + \mathsf{U}_z = \sum_\sigma n_{f\sigma} - 2n_h \tag{8.2}$$

[see Eqs. (3.25), (4.2), and (8.1)].

J. Hubbard in his pioneering papers[30–33] warned us against decoupling the single-site correlations in the Green functions containing the X operators. One may say that the mean-field decoupling of Hubbard operators is a crude violation of this commandment, which breaks the intrinsic symmetry of strongly correlated electron systems and results in multiple artifacts in description of these quantum objects. We hope that the use of Gell-Mann representation will pave the way for construction of diagrammatic techniques free from such shortcomings. Besides, the simple form of the Anderson Hamiltonian in Gell-Mann representation, (3.21)–(3.26) may facilitate formulation of low-energy field theories, especially, for the system with charge-spin separation.

We considered in this paper only the dynamical symmetries of nondegenerate Hubbard atom. Similar approach may be used for the models including orbital variables (double quantum dots and two-well traps, in general). In that case, one deals with the spin $\vec{\sigma}$ and pseudospin $\vec{\tau}$ variables, and the interlevel transitions also obey the $SU(4)$ dynamical symmetry groups.[69] If the two-trap well is occupied by the spinless objects (e.g., cold atoms), the corresponding dynamical symmetry is $SU(3)$.[70] In these situations, the Gell-Mann matrices do not reflect the nature of excitation spectra, and other matrix representations of $SU(n)$ groups should be used. But in all cases, the group generators may be constructed by means of appropriate Hubbard operators.

The general picture of dynamical symmetries includes not only the nano-objects with local $SU(n)$ symmetries in the subspaces Φ_n with variable occupation numbers $\mathcal{N}$ but also the objects with local symmetries $SO(n)$ existing in the subspaces $\Xi_n = \{S, T, E_{iS}, E_{iT}\}$ with fixed even $\mathcal{N}$, where S and T are spin singlet and spin triplet and E_{iS} and E_{iT} are various singlet and triplet charge transfer excitons, respectively. Numerous physical manifestations of these symmetries are described in Ref. 71.

APPENDIX: GELL-MANN MATRICES AND HUBBARD OPERATORS

Here, we summarize for the sake of convenience some properties of the Gell-Mann matrices of 4th rank and their realization in the Hubbard and Anderson models. The canonical form of these matrices describing the symmetry of four-level systems is

$$\lambda_1 = \begin{pmatrix} 0 & 1 & 0 & 0 \\ 1 & 0 & 0 & 0 \\ 0 & 0 & 0 & 0 \\ 0 & 0 & 0 & 0 \end{pmatrix}, \quad \lambda_2 = \begin{pmatrix} 0 & -i & 0 & 0 \\ i & 0 & 0 & 0 \\ 0 & 0 & 0 & 0 \\ 0 & 0 & 0 & 0 \end{pmatrix}, \quad \lambda_3 = \begin{pmatrix} 1 & 0 & 0 & 0 \\ 0 & -1 & 0 & 0 \\ 0 & 0 & 0 & 0 \\ 0 & 0 & 0 & 0 \end{pmatrix}, \quad \lambda_4 = \begin{pmatrix} 0 & 0 & 1 & 0 \\ 0 & 0 & 0 & 0 \\ 1 & 0 & 0 & 0 \\ 0 & 0 & 0 & 0 \end{pmatrix},$$

$$\lambda_5 = \begin{pmatrix} 0 & 0 & -i & 0 \\ 0 & 0 & 0 & 0 \\ i & 0 & 0 & 0 \\ 0 & 0 & 0 & 0 \end{pmatrix}, \quad \lambda_6 = \begin{pmatrix} 0 & 0 & 0 & 0 \\ 0 & 0 & 1 & 0 \\ 0 & 1 & 0 & 0 \\ 0 & 0 & 0 & 0 \end{pmatrix}, \quad \lambda_7 = \begin{pmatrix} 0 & 0 & 0 & 0 \\ 0 & 0 & -i & 0 \\ 0 & i & 0 & 0 \\ 0 & 0 & 0 & 0 \end{pmatrix}, \quad \lambda_8 = \frac{1}{\sqrt{3}} \begin{pmatrix} 1 & 0 & 0 & 0 \\ 0 & 1 & 0 & 0 \\ 0 & 0 & -2 & 0 \\ 0 & 0 & 0 & 0 \end{pmatrix},$$

$$\lambda_9 = \begin{pmatrix} 0 & 0 & 0 & 1 \\ 0 & 0 & 0 & 0 \\ 0 & 0 & 0 & 0 \\ 1 & 0 & 0 & 0 \end{pmatrix}, \quad \lambda_{10} = \begin{pmatrix} 0 & 0 & 0 & -i \\ 0 & 0 & 0 & 0 \\ 0 & 0 & 0 & 0 \\ i & 0 & 0 & 0 \end{pmatrix}, \quad \lambda_{11} = \begin{pmatrix} 0 & 0 & 0 & 0 \\ 0 & 0 & 0 & 1 \\ 0 & 0 & 0 & 0 \\ 0 & 1 & 0 & 0 \end{pmatrix}, \quad \lambda_{12} = \begin{pmatrix} 0 & 0 & 0 & 0 \\ 0 & 0 & 0 & -i \\ 0 & 0 & 0 & 0 \\ 0 & i & 0 & 0 \end{pmatrix},$$

$$\lambda_{13} = \begin{pmatrix} 0 & 0 & 0 & 0 \\ 0 & 0 & 0 & 0 \\ 0 & 0 & 0 & 1 \\ 0 & 0 & 1 & 0 \end{pmatrix}, \quad \lambda_{14} = \begin{pmatrix} 0 & 0 & 0 & 0 \\ 0 & 0 & 0 & 0 \\ 0 & 0 & 0 & -i \\ 0 & 0 & i & 0 \end{pmatrix}, \quad \lambda_{15} = \frac{1}{\sqrt{6}} \begin{pmatrix} 1 & 0 & 0 & 0 \\ 0 & 1 & 0 & 0 \\ 0 & 0 & 1 & 0 \\ 0 & 0 & 0 & -3 \end{pmatrix}, \tag{A1}$$

(see, e.g., Ref. 72). First eight matrices contain the 3rd rank Gell-Mann operators of the $SU(3)$ group as submatrices. The operators λ_9–λ_{15} generate transitions between the triplet and the fourth level.

Each nonzero matrix element in λ_i represents one of the Hubbard operators $X^{\Lambda\Lambda'}$ acting in the space Φ_4 (3.5). Using this mapping, we find the inverse representation of Hubbard operators via the Gell-Mann matrices:

$$X^{\uparrow 0} = \frac{1}{2}(\lambda_4 + i\lambda_5), \quad X^{0\uparrow} = \frac{1}{2}(\lambda_4 - i\lambda_5), \quad X^{\downarrow 0} = \frac{1}{2}(\lambda_6 + i\lambda_7), \quad X^{0\downarrow} = \frac{1}{2}(\lambda_6 - i\lambda_7)/2,$$

$$X^{2\uparrow} = \frac{1}{2}(\lambda_9 - i\lambda_{10}), \quad X^{\uparrow 2} = \frac{1}{2}(\lambda_9 + i\lambda_{10}), \quad X^{2\downarrow} = \frac{1}{2}(\lambda_{11} - i\lambda_{12}), \quad X^{\downarrow 2} = \frac{1}{2}(\lambda_{11} + i\lambda_{12}),$$

$$X^{\uparrow\downarrow} = \frac{1}{2}(\lambda_1 + i\lambda_2), \quad X^{\downarrow\uparrow} = \frac{1}{2}(\lambda_1 - i\lambda_2), \quad X^{20} = \frac{1}{2}(\lambda_{13} - i\lambda_{14}), \quad X^{02} = \frac{1}{2}(\lambda_{13} + i\lambda_{14}),$$

$$X^{\uparrow\uparrow} = \frac{1}{4}\left(1 + 2\lambda_3 + \frac{2}{\sqrt{3}}\lambda_8 + \frac{2}{\sqrt{6}}\lambda_{15}\right), \quad X^{\downarrow\downarrow} = \frac{1}{4}\left(1 - 2\lambda_3 + \frac{2}{\sqrt{3}}\lambda_8 + \frac{2}{\sqrt{6}}\lambda_{15}\right),$$
$$X^{00} = \frac{1}{4}\left(1 - \frac{4}{\sqrt{3}}\lambda_8 + \frac{2}{\sqrt{6}}\lambda_{15}\right), \quad X^{22} = \frac{1}{4}(1 - \sqrt{6}\lambda_{15}). \tag{A2}$$

One may construct a subgroup $SU(2)$ of the group $SU(n)$ for any 2D subspace of the effective Fock space. There are three such "triads" grouped in three vectors $\vec{\mathsf{T}}$, $\vec{\mathsf{U}}$, and $\vec{\mathsf{V}}$ for the group $SU(3)$ with the symmetry operations acting in the 3D space $\bar{\Phi}_3$ (cf. Ref. 48). Adding fourth dimension provides three more vectors $\vec{\mathsf{W}}$, $\vec{\mathsf{Y}}$, and $\vec{\mathsf{Z}}$ representing the generators of the group $SU(4)$ together with the first three vectors:

$$\mathsf{T}^{\pm} = \frac{1}{2}(\lambda_1 \pm i\lambda_2), \quad \mathsf{T}_z = \lambda_3, \quad \mathsf{U}^{\pm} = \frac{1}{2}(\lambda_6 \pm i\lambda_7), \quad \mathsf{U}_z = \frac{1}{2}(-\lambda_3 + \sqrt{3}\lambda_8),$$
$$\mathsf{V}^{\pm} = \frac{1}{2}(\lambda_4 \pm i\lambda_5), \quad \mathsf{V}_z = \frac{1}{2}(\lambda_3 + \sqrt{3}\lambda_8), \quad \mathsf{W}^{\pm} = \frac{1}{2}(\lambda_9 \pm i\lambda_{10}), \quad \mathsf{W}_z = \frac{1}{2}\left(\lambda_3 + \frac{1}{\sqrt{3}}\lambda_8 + \frac{4}{\sqrt{6}}\lambda_{15}\right), \tag{A3}$$
$$\mathsf{Y}^{\pm} = \frac{1}{2}(\lambda_{11} \pm i\lambda_{12}), \quad \mathsf{Y}_z = \frac{1}{2}\left(-\lambda_3 + \frac{1}{\sqrt{3}}\lambda_8 + \frac{4}{\sqrt{6}}\lambda_{15}\right), \quad \mathsf{Z}^{\pm} = \frac{1}{2}(\lambda_{13} \pm i\lambda_{14}), \quad \mathsf{Z}_z = \frac{1}{\sqrt{3}}(-\lambda_8 + \sqrt{2}\lambda_{15}).$$

The operators $\mathsf{T}^{\pm}$ and T_z from the first triad in the set (A3) describe the spin-flip excitations in the homopolar subspace $\mathcal{N} = 1$ of the Hubbard atom. The operators $\mathsf{Z}^{\pm}$ and Z_z from the last triad may be used in the description of excitations in the two-particle sector $\mathcal{N} = \{0,2\}$ of the Hubbard and Anderson models. The operators forming the triads $\vec{\mathsf{U}}$ and $\vec{\mathsf{V}}$ intermix the states from the charge sectors $\mathcal{N} = 0$ and 1, and the operators $\vec{\mathsf{W}}$ and $\vec{\mathsf{Y}}$ do the same for the sectors $\mathcal{N} = 2$ and 1 [see Eq. (3.13)].

In many physical applications, the reduced Anderson and Hubbard Hamiltonians with $U \to \infty$ are exploited. In this limit, the doubly occupied state $|2\rangle$ is completely suppressed. In the appropriately reduced Fock space $\bar{\Phi}_3$ (3.7) possessing the $SU(3)$ symmetry, the system (A2) transforms into

$$X^{\uparrow 0} = \frac{1}{2}(\lambda_4 + i\lambda_5), \quad X^{0\uparrow} = \frac{1}{2}(\lambda_4 - i\lambda_5), \quad X^{\downarrow 0} = \frac{1}{2}(\lambda_6 + i\lambda_7), \quad X^{0\downarrow} = \frac{1}{2}(\lambda_6 - i\lambda_7)/2,$$
$$X^{\uparrow\downarrow} = \frac{1}{2}(\lambda_1 + i\lambda_2), \quad X^{\downarrow\uparrow} = \frac{1}{2}(\lambda_1 - i\lambda_2), \quad X^{\uparrow\uparrow} = \frac{1}{2}\left(\frac{2}{3} + \lambda_3 + \frac{1}{\sqrt{3}}\lambda_8\right), \quad X^{\downarrow\downarrow} = \frac{1}{2}\left(\frac{2}{3} - \lambda_3 + \frac{1}{\sqrt{3}}\lambda_8\right), \tag{A4}$$
$$X^{00} = \frac{1}{3}(1 - \sqrt{3}\lambda_8).$$

Within each triad the standard Pauli commutation relations (3.27) for the components are valid. The commutation relations between the operators from different subgroups are described by more complicated structure factors.[48] These relations in our case may be derived from the general commutation relations (2.7) for the Hubbard operators (see the main text).

Two diagonal matrices entering the Hamiltonian (3.20) are

$$\mathsf{Q}_z = \begin{pmatrix} 1 & 0 & 0 & 0 \\ 0 & 1 & 0 & 0 \\ 0 & 0 & -2 & 0 \\ 0 & 0 & 0 & 0 \end{pmatrix}, \quad \mathsf{P}_z = \begin{pmatrix} 1 & 0 & 0 & 0 \\ 0 & 1 & 0 & 0 \\ 0 & 0 & 0 & 0 \\ 0 & 0 & 0 & -2 \end{pmatrix}. \tag{A5}$$

[see also Eq. (4.4)].

[1] Y. Ne'eman, Nucl. Phys. **26**, 222 (1961).
[2] M. Gell-Mann, Phys. Lett. **8**, 214 (1964).
[3] G. Zweig CERN Reports No. 8181/Th 8419, 8419/Th 8412 (1964).
[4] M. Gell-Mann and Y. Ne'eman, *The Eightfold Way* (Westview Press, 1964).
[5] A. O. Barut, Phys. Rev. **135**, B839 (1964).
[6] Y. Dothan, M. Gell-Mann, and Y. Ne'eman, Phys. Lett. **17**, 148 (1965).
[7] M. J. Englefield, *Group Theory and the Coulomb Problem* (Wiley, New York, 1972).
[8] I. A. Malkin and V. I. Man'ko, *Dynamical Symmetries and Coherent States of Quantum Systems* (Nauka, Moscow, 1979).
[9] N. Mukunda, L. O'Raifeartaigh, and E. C. G. Sudarshan, Phys. Rev. Lett. **15**, 1041 (1965).
[10] E. C. G. Sudarshan, N. Mukunda, and L. O'Raifeartaigh, Phys. Lett. **19**, 322 (1965).
[11] I. A. Malkin and V. I. Man'ko, Pis'ma Zh. Eksp. Teor. Fiz. **2**, 230 (1965) [JETP Lett. **2**, 146 (1965)]; Jadernaya Fizika **3**, 372 (1966) [Sov. J. Nucl. Phys. **3**, 267 (1966)].
[12] S. Goshen and H. J. Lipkin, Ann. Phys. **6**, 301 (1959).

[13]A. O. Barut, Phys. Rev. **139**, B1433 (1965).
[14]R. C. Hwa and J. Nuyts, Phys. Rev. **145**, 1188 (1966).
[15]L. P. Kouwenhoven, D. G. Austing, and S. Tarucha, Rep. Progr. Phys. **64**, 701 (2001).
[16]P. H. Sachrajda and M. Ciorga, *Nano-spintronics with Lateral Quantum Dots* (Kluwer, Boston, 2003).
[17]*Molecular Electronics*, edited by G. Cuniberti, G. Fagas, and K. Richter, Lecture Notes in Physics Vol. 680 (Springer, Berlin, 2005).
[18]D. Natelson, *Handbook of Organic Electronics and Photonics* (American Scientific Publishers, Valencia, 2006).
[19]R. Hanson, L. P. Kouwenhoven, J. R. Petta, S. Tarucha, and L. M. K. Vandersypen, Rev. Mod. Phys. **79**, 1217 (2007).
[20]P. W. Anderson, J. Phys. C: Solid. State Phys. **3**, 2436 (1970).
[21]A. A. Abrikosov and A. B. Migdal, J. Low Temp. Phys. **3**, 519 (1970).
[22]M. Fowler and A. Zawadowski, Solid State Commun. **9**, 471 (1971).
[23]J. H. Jefferson, J. Phys. C: Solid. State Phys. **10**, 3589 (1977).
[24]F. D. M. Haldane, Phys. Rev. Lett. **40**, 416 (1978).
[25]P. B. Wiegmann and A. M. Tsvelik, J. Phys. C.: Solid St. Phys. **16**, 2281 (1983).
[26]N. Kawakami and A. Okiji, Phys. Rev. B **42**, 2383 (1990).
[27]H.-B. Schüttler and A. J. Fedro, Phys. Rev. B **38**, 9063 (1988).
[28]A. Taraphder and P. Coleman, Phys. Rev. Lett. **66**, 2814 (1991).
[29]*The One-dimensional Hubbard Model*, edited by F. H. L. Essler, H. Frahm, A. Klümper, and V. E. Korepin (Cambridge University Press, Cambridge, 2005).
[30]J. Hubbard, Proc. Roy. Soc. A **276**, 238 (1963).
[31]J. Hubbard, Proc. Roy. Soc. A **277**, 237 (1964).
[32]J. Hubbard, Proc. Roy. Soc. A **281**, 401 (1964).
[33]J. Hubbard, Proc. Roy. Soc. A **285**, 542 (1965).
[34]P. B. Wiegmann, Phys. Rev. Lett. **60**, 821 (1988).
[35]A. Foerster and M. Karowski, Phys. Rev. B **46**, 9234 (1992).
[36]L. I. Glazman and M. E. Raikh, Pis'ma Zh. Eksp. Teor. Fiz. **47**, 378 (1988) [JETP Lett. **47**, 452 (1988)].
[37]T. K. Ng and P. A. Lee, Phys. Rev. Lett. **61**, 1768 (1988).
[38]A. M. Tsvelik and P. B. Wiegmann, Adv. Phys. **32**, 453 (1983).
[39]N. Andrei, F. Furuya, and J. H. Loewenstein, Rev. Mod. Phys. **55**, 331 (1983).
[40]P. W. Anderson, Phys. Rev. Lett. **18**, 1049 (1967).
[41]D. Giuliano and A. Tagliacozzo, Phys. Rev. Lett. **84**, 4677 (2000); D. Guiliano, B. Jouault, and A. Tagliacozzo, Phys. Rev. B **63**, 125318 (2001).
[42]M. Eto and Yu.V. Nazarov, Phys. Rev. Lett. **85**, 1306 (2000); Phys. Rev. B **64**, 085322 (2001).
[43]K. Kikoin and Y. Avishai, Phys. Rev. Lett. **86**, 2090 (2001); Phys. Rev. B **65**, 115329 (2002).
[44]T. Kuzmenko, K. Kikoin, and Y. Avishai, Phys. Rev. Lett. **89**, 156602 (2002); Phys. Rev. B **69**, 195109 (2004).
[45]K. Kikoin, Y. Avishai, and M. N. Kiselev, *Dynamical Symmetries in Nanophysics*, in Nanophysics, Nanoclusters and Nanodevices (Nova Science Publishers, New York, 2006), pp. 39–86.
[46]J. R. Schrieffer and P. A. Wolff, Phys. Rev. **149**, 491 (1966).
[47]Yu. A. Izyumov, and Yu. N. Skryabin, *Statistical Mechanics of Magnetically Ordered Systems* (Plenum, New York, 1988).
[48]J. Elliot and P. Dauber, *Symmetry in Physics* (Macmillan, London, 1979), Chap. 11.
[49]P. W. Anderson, Phys. Rev. Lett. **34**, 953 (1975).
[50]I. G. Lang and Yu. A. Firsov, Sov. Phys. JETP **16**, 1301 (1963) [Zh. Eksp. Teor. Phys. **43**, 1843 (1962)].
[51]P. S. Cornaglia, D. R. Grempel, and H. Ness, Phys. Rev. B **71**, 075320 (2005).
[52]P. S. Cornaglia and D. R. Grempel, Phys. Rev. B **71**, 245326 (2005).
[53]A. S. Alexandrov, A. M. Bratkovsky, and R. S. Williams, Phys. Rev. B **67**, 075301 (2003).
[54]J. Koch, M. E. Raikh, and F. von Oppen, Phys. Rev. Lett. **96**, 056803 (2006).
[55]J. Koch, E. Sela, Y. Oreg, and F. von Oppen, Phys. Rev. B **75**, 195402 (2007).
[56]M. Leijnse, M. R. Wegewijs, and M. H. Hettler, Phys. Rev. Lett. **103**, 156803 (2009).
[57]J.-S. Lim, R. Lopez, G.-L. Giorgi, and D. Sanchez, Phys. Rev. B **83**, 155325 (2011).
[58]F. D. M. Haldane and P. W. Anderson, Phys. Rev. B **13**, 2553 (1976).
[59]V. N. Fleurov and K. A. Kikoin, J. Phys. C **9**, 1673 (1976).
[60]K. A. Kikoin and V. N. Flerov, Zh. Eksp. Teor. Phys. **77**, 1062 (1979) [Sov. Phys. JETP **50**, 535 (1979)].
[61]G. Cohen, V. Fleurov, and K. Kikoin, Phys. Rev. B **79**, 245307 (2009).
[62]C. N. Yang and S. C. Zhang, Mod. Phys. Lett. B **4**, 759 (1990); S. C. Zhang, Int J. Mod. Phys. **5**, 153 (1991).
[63]A. Masumizu and K. Sogo, Phys. Rev. B **72**, 115107 (2005).
[64]N. Read and D. M. Newns, J. Phys. C **16**, 3273 (1983).
[65]P. Coleman, Phys. Rev. B **29**, 3035 (1984).
[66]I. Affleck and J. B. Marston, Phys. Rev. B **37**, 3774 (1988).
[67]M. N. Kiselev, H. Feldmann, and R. Oppermann, Eur. Phys. J. B **22**, 53 (2001).
[68]Yu. Kagan, K. A. Kikoin, and N. V. Prokof'ev, Physica B **182**, 201 (1992).
[69]M. Eto, J. Phys. Soc. Jpn. **74**, 95 (2005).
[70]K. Kikoin, M. N. Kiselev, and A. L. Chudnovskiy (unpublished).
[71]K. Kikoin, M. N. Kiselev, and Y. Avishai, *Dynamical Symmetries for Nanostructures* (Springer, Wien, 2012).
[72]T. Tilma, M. Byrd, and E. C. G. Sudarshan, J. Phys. A: Math. Gen. **35**, 10445 (2002).